Journal of Theoretical Biology 497 (2020) 110265

Contents lists available at ScienceDirect

Journal of Theoretical Biology

journal homepage: www.elsevier.com/locate/jtb

Modeling the waning and boosting of immunity from infection or vaccination☆

Rose-Marie Carlsson[a], Lauren M Childs[b], Zhilan Feng[c,d], John W Glasser[e], Jane M Heffernan[f,*], Jing Li[g], Gergely Röst[h]

[a] Public Health Agency of Sweden, Solna, Sweden
[b] Virginia Tech, Blacksburg, VA, USA
[c] Purdue University, West Lafayette, IN, USA
[d] National Science Foundation, Alexandria, VA, USA
[e] Centers for Disease Control and Prevention, Atlanta, GA, USA
[f] York University, Toronto, ON, Canada
[g] California State University, Northridge, CA, USA
[h] University of Szeged, Szeged, Hungary

ARTICLE INFO

Article history:
Received 1 October 2019
Revised 13 March 2020
Accepted 1 April 2020
Available online 6 April 2020

MSC:
92D25
92D30

Keywords:
Mathematical epidemiology
Waning and boosting of immunity
Vaccination
Age- and immunity-structured population
Immuno-epidemiology

ABSTRACT

Immunity following natural infection or immunization may wane, increasing susceptibility to infection with time since infection or vaccination. Symptoms, and concomitantly infectiousness, depend on residual immunity. We quantify these phenomena in a model population composed of individuals whose susceptibility, infectiousness, and symptoms all vary with immune status. We also model age, which affects contact, vaccination and possibly waning rates. The resurgences of pertussis that have been observed wherever effective vaccination programs have reduced typical disease among young children follow from these processes. As one example, we compare simulations with the experience of Sweden following resumption of pertussis vaccination after the hiatus from 1979 to 1996, reproducing the observations leading health authorities to introduce booster doses among school-aged children and adolescents in 2007 and 2014, respectively. Because pertussis comprises a spectrum of symptoms, only the most severe of which are medically attended, accurate models are needed to design optimal vaccination programs where surveillance is less effective.

1. Introduction

Hosts may have immunological memory following vaccination or recovery from infection that protects from subsequent disease if not infection. If T- or B- cell populations decay, as they do against most bacterial and some viral pathogens, immunity declines, but can be boosted by re-vaccination or subsequent infection. Hosts with insufficient immunity to protect them from disease may experience moderate or mild symptoms and be concomitantly less infectious than fully susceptible hosts who experience typical disease Mims et al. (2001).

Mathematical models have been used to study the effects of vaccination Anderson and May (1982), age Anderson and May (1985), and waning of immunity Mossong et al. (1999) on the dynamics and persistence of infectious diseases. The importance of the boosting of immunity corresponding to sub-clinical infection in individuals whose immunity has waned has also been identified Glass and Grenfell (2003). Boosting of immunity by re-exposure prolongs the period of protection, but may also maintain oscillations in the prevalence of disease Lavine et al. (2011).

Several theoretical papers have been devoted to understanding the dynamical consequences of immune system boosting. Their authors use various mathematical approaches: ordinary differential equations Dafilis et al. (2012), partial differential equations Barbarossa and Röst (2015), delay differential equations Barbarossa et al., 2017, and renewal equations Diekmann et al. (2018). Biolog-

☆ Authors contributed equally. None has competing interests. The findings and conclusions in this report do not necessarily represent official positions of the Centers for Disease Control and Prevention, National Science Foundation, or other institutions with which the authors are affiliated. Simulation code will be posted to github upon acceptance.

* Corresponding author.
E-mail address: jmheffer@yorku.ca (J.M. Heffernan).

https://doi.org/10.1016/j.jtbi.2020.110265

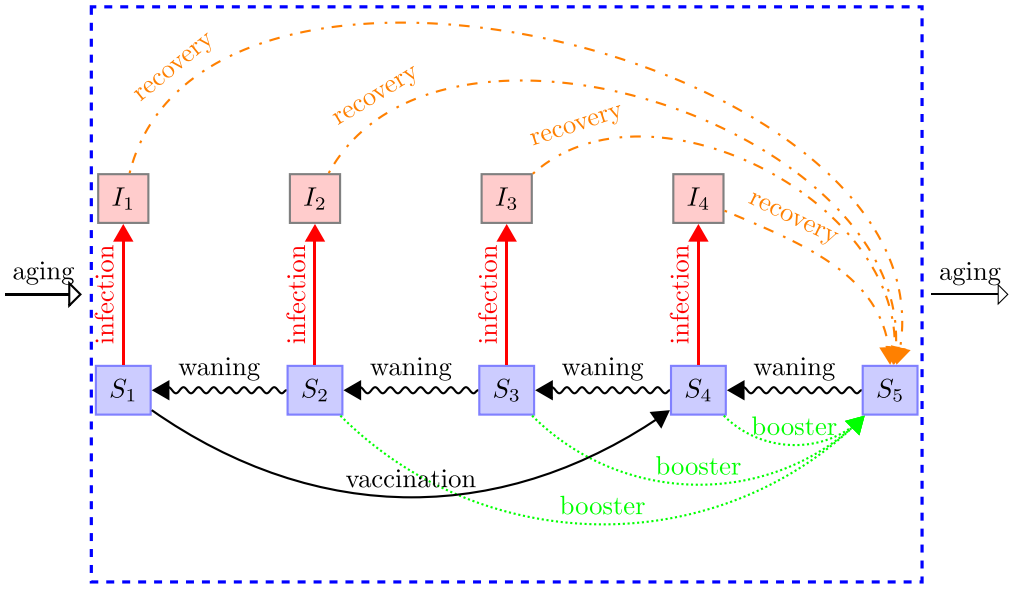

Fig. 1. Schematic of the PDE system given in Eq. (2)-Eq. (4) for one age group. S_1, S_2, S_3, S_4, and S_5 (blue shaded boxes) represent susceptible individuals who are immunologically naive, have some immunity, are moderately immune, were recently vaccinated, and are fully immune, respectively. I_1, I_2, I_3, and I_4 (red shaded boxes) represent infected individuals with typically severe symptoms who are maximally infectious, moderate symptoms and reduced infectiousness, mild symptoms and even less infectiousness, and neither symptoms nor infectiousness, respectively (we set $I_5 = 0$ in the text for ease of notation). Recovery from disease leads to a fully immune state (orange dash-dotted line). As individuals age, susceptible ones with incomplete immunity, including naive (S_1), some (S_2), moderate (S_3), and vaccine-induced (S_4) immunity, can be infected (red solid line) and become infectious. After infection, they recover (dot-dashed orange lines) fully immune (S_5). However, as individuals age, their immunity wanes (black wavy lines). The immunologically naive group (S_1) can become immune (S_4) through primary or re-vaccination (black solid line). Groups with some (S_2), moderate (S_3), and vaccine-induced immunity (S_4) can become fully immune (S_5) through re-vaccination (green dotted lines) . (For interpretation of the references to colour in this figure legend, the reader is referred to the web version of this article.)

ical assumptions on the nature of boosting also influence disease dynamics Heffernan and Keeling, 2009; Barbarossa et al., 2018; Leung et al. (2018).

We are interested in quantifying the distribution of host population immunity and effects of immunity-modified disease on the spread and persistence of pathogens in host populations. Immune system memory and response dynamics may change with age as fewer naive T-cells remain to be programmed to respond to particular antigens Mims et al. (2001). As the force of infection also varies with age, symptom severity and infectiousness may vary too. In addition, vaccination programs usually are age-specific. It is thus necessary to consider the effects of host age in studies of the waning and boosting of immunity.

Accordingly, we study a model that involves host age and immune status, which determine symptoms and concomitant infectiousness. Our model consists of a system of partial differential equations that track susceptible, vaccinated and infected hosts over time in defined age and immune classes. The model is applicable to many diseases, including that caused by *B. pertussis*, which we examine as a proof-of-principle application.

Several age-structured models of pertussis transmission dynamics have been proposed (e.g., Hethcote (1997, 1999); Campbell et al. (2015)). The authors of these and many subsequent articles use multiple epidemiological classes to account for recovered and vaccinated individuals with different levels of immunity and infected individuals experiencing more or less severe symptoms. Our model has a simpler epidemiological structure (fewer compartments), yet is consistent with the underlying immunological processes, and allows us to include various levels of immunity, re-vaccination, and boosting by natural exposure. Previous modelers also assumed that individuals differing in immune status share the same susceptibility, and hence that the force of infection is uniform within age groups. To better reflect immunological knowledge, susceptibility depends on immune status in our model.

Despite the existence of safe and effective vaccines, pertussis (whooping cough) continues to affect human populations around the globe. After effective childhood vaccination programs markedly reduced typical disease among young children, outbreaks were observed among adolescents, generally of immunity-modified disease. Explanations for these resurgences range from secular changes in mixing patterns and other social phenomena Águas et al., 2006; Rohani et al. (2010) to deficiencies in immunity induced by the acellular vaccines licensed decades ago Gambhir et al., 2015.

An alternative is that effective routine vaccination programs, initially with the whole-cell vaccine, unmasked the waning of natural immunity that had been boosted by the exposure of older children to infectious younger ones. People with mild symptoms rarely seek care, but – because symptom severity depends on immunity, a function of time since vaccination or most recent exposure – by the time that adolescents were exposed, their immunity was no longer able to protect them from clinical disease.

We apply our model of the waning and boosting of immunity to pertussis in Sweden after the 17-year hiatus in vaccination during which clinical trials of the current generation of acellular vaccines were conducted Olin et al., 1997; Storsaeter et al., 1990; Trollfors et al. (1995); Gustafsson et al. (1996). Because vaccination changes the epidemiology of disease, programs must be dynamic. We evaluate Swedish health authorities' decisions about re-vaccination and, coincidentally, test our explanation for the resurgence.

2. The model

2.1. Model formulation

We track individual age, infection and immune status by modeling ages 0–19 years in single year groups, 20–44 years in 5-year groups, 45–74 years in 10-year groups, 75+ years (a total of 29 age groups) in a single group, and several susceptible (S) and

Table 1
Variables and parameters used in the PDE system given in Eqs. (2), (3), and (4). Immune status is classified as immunologically naive, somewhat immune, moderately immune, recently vaccinated, and completely immune. There are only four infectious classes as S_5 is completely immune. For the ODE system, similar variables are used for $S_{in}(t)$ and $I_{jn}(t)$ with i, j $(1 \le i \le 5,\ 1 \le j \le 4)$ indexing immune status and n age groups.

Variable description	Symbol
Fully susceptible (naive)	$S_1(a,\ t)$
Susceptible with limited immunity	$S_2(a,\ t)$
Susceptible with moderate immunity	$S_3(a,\ t)$
Susceptible with vaccine-induced immunity	$S_4(a,\ t)$
Complete immunity (resistant)	$S_5(a,\ t)$
Infected with severe disease	$I_1(a,\ t)$
Infected with moderate disease	$I_2(a,\ t)$
Infected with mild disease	$I_3(a,\ t)$
Infected, but asymptomatic	$I_4(a,\ t)$
Total population of status j	$T_j(a,t) = S_j(a,t) + I_j(a,t),\ 1 \le j \le 4$ $T_5(a,t) = S_5(a,t)$
Parameter description	**Symbol**
Susceptibility of individuals of immune status i, age a	$\alpha_i(a)$
Infectivity of individuals of immune status i, age a	$\beta_i(a)$
Activity rate of age a	$A(a)$
Waning rate of individuals of immune status i	$\omega_i(a)$
Vaccination rate of individuals of immune status i, age group a	$\rho_i(a)$
Recovery rate of infected individuals of immune status i, age a	$\gamma_i(a)$
Birth rate of individuals aged a	$f(a)$
Natural mortality rate of individuals aged a	$\mu(a)$
Contacts between individuals aged a and θ	$c(a,\ \theta)$
Proportion of the contacts between individuals aged a and those of immune status i, age θ	$c_i(a,\ \theta)$

infected (I) states. A schematic is provided in Fig. 1 for one age group. We distinguish 5 immune classes (fully susceptible, somewhat immune, moderately immune, recently vaccinated, fully resistant to infection), and assume not only that individuals of higher immune status are less susceptible to infection than those of lower status, but that that, if infected, higher status individuals will develop milder symptoms and be correspondingly less infectious. Immunity develops after primary and re-vaccination (black solid and green dotted lines, respectively) and infection (orange dot dashed lines), but wanes (black wavy lines).

We use $S_i(a,\ t)$ and $I_i(a,\ t)$ to denote the density of susceptible and infected individuals aged a $(0 \le a < \infty)$ with immune status i $(1 \le i \le 5)$ at time t. The total population of individuals of age a and immune status i is denoted by $T_i(a,\ t)$, the sum of $S_i(a,\ t)$ and $I_i(a,\ t)$,

$$T_i(a,t) = S_i(a,t) + I_i(a,t), \quad 1 \le j \le 4, \quad \text{and} \quad T_5(a,t) = S_5(a,t).$$

Here, for the S group, $i = 1, ., 5$, but for the I group, $1 \le i \le 4$ because those in S_5 are fully immune (Table 1). Immunity wanes at rate $\omega_i(a)$ for immune status i. Susceptible individuals who are immunologically naive, $S_1(a)$, can be vaccinated (primary series typically consist of multiple doses) and acquire vaccine-induced immunity, $S_4(a)$. Individuals who are immunologically naive, have some, moderate, and vaccine-induced immunity, $S_1(a)$, $S_2(a)$, $S_3(a)$ and $S_4(a)$, respectively, can receive booster vaccine doses, by which they acquire complete immunity, $S_5(a)$, at rate $\rho_i(a)$ $(1 \le i \le 4$, respectively). The groups of susceptible individuals, $S_i(a,\ t)$, $(1 \le i \le 4)$, are assumed to have susceptibility $\alpha_i(a)$ and contact rate $A(a)$ at age a. Individuals can be infected at rate $\beta_j(a)$ by infectious individuals from immunity class j $(1 \le j \le 4)$. We use a mixing function $c(a,\ \theta)$ to represent how the contacts of an individual aged a are distributed among individuals of age θ. Hence,

$$\int_0^\infty c(a,\theta)d\theta = 1, \quad \text{for any} \quad a \ge 0,$$

and

$$\int_{\theta_1}^{\theta_2} c(a,\theta)d\theta, \quad \text{for} \quad \theta_2 > \theta_1 \ge 0,$$

expresses the proportion of the contacts of an individual aged a with individuals between ages θ_1 and θ_2. To further describe how many of these contacts are with individuals of immune class j $(1 \le j \le 4)$ and age θ, we introduce $c_j(a,\ \theta,\ t)$ as follows:

$$c_j(a,\theta,t) := \frac{T_j(\theta,t)}{\sum_{j=1}^{5} T_j(\theta,t)} c(a,\theta). \tag{1}$$

Infected individuals $I_i(a,\ t)$ recover from disease at rate $\gamma_i(a)$.

We assume that members of the population aged a have death rate $\mu(a)$, and have offspring (entering class $S_1(0,\ t)$) at birth rate $f(a)$. Therefore, we consider the system of equations

$$\begin{aligned}
&\underbrace{\frac{\partial S_i(a,t)}{\partial t} + \frac{\partial S_i(a,t)}{\partial a}}_{\text{Susceptible classes: } 1\le i\le 4} \\
&= -\underbrace{\alpha_i(a)A(a)S_i(a,t)\lambda(a,t)}_{\text{loss of susceptibility due to infection}} \\
&-\underbrace{\mu(a)S_i(a,t)}_{\text{natural death}} + \underbrace{\omega_{i+1}(a)S_{i+1}(a,t)}_{\text{waning into class}} - \underbrace{\omega_i(a)S_i(a,t)}_{\text{waning out of class}} \\
&+ \underbrace{\psi_i\rho_1(a)S_1(a,t)}_{\text{immunity acquired by vaccination}} - \underbrace{\rho_i(a)S_i(a,t)}_{\text{loss of susceptibility by vaccination}}
\end{aligned} \tag{2}$$

$$\begin{aligned}
&\underbrace{\frac{\partial S_5(a,t)}{\partial t} + \frac{\partial S_5(a,t)}{\partial a}}_{\text{Completely immune class } (i=5)} \\
&= -\underbrace{\mu(a)S_5(a,t)}_{\text{natural death}} - \underbrace{\omega_5(a)S_5(a,t)}_{\text{waning out of class}} \\
&+ \underbrace{\sum_{j=1}^{4}\gamma_j(a)I_j(a,t)}_{\text{immunity acquired by infection}} + \underbrace{\sum_{j=2}^{4}\rho_j(a)S_j(a,t)}_{\text{immunity acquired by booster dose}}
\end{aligned} \tag{3}$$

$$\underbrace{\frac{\partial I_i(a,t)}{\partial t}+\frac{\partial I_i(a,t)}{\partial a}}_{\text{Infected classes: } 1\le i\le 4} = \underbrace{\alpha_i(a)A(a)S_i(a,t)\lambda(a,t)}_{\text{entering infected class due to infection}} - \underbrace{\mu(a)I_i(a,t)}_{\text{natural death}} - \underbrace{\gamma_i(a)I_i(a,t)}_{\text{recovery}} \tag{4}$$

$$\lambda(a,t)=\sum_{j=1}^{4}\int_0^\infty \frac{c_j(a,\theta,t)\beta_j(\theta)I_j(\theta,t)}{T_j(\theta,t)}d\theta, \tag{5}$$

with the following boundary conditions:

$$I_i(0,t)=0, \qquad \text{for } 1\le i\le 4,$$

$$S_1(0,t)=\sum_{j=1}^{5}\int_0^\infty f(\theta)\big[S_j(\theta,t)+I_j(\theta,t)\big]d\theta,$$

$$S_i(0,t)=0, \qquad \text{for } 2\le i\le 5,$$

and constraints

$$\psi_i=\begin{cases}1, & \text{if } i=4,\\ 0, & \text{otherwise,}\end{cases} \tag{6}$$

and

$$\omega_1(a)=0, \tag{7}$$

where i and j refer to immune status. Here, the function ψ is introduced for notational convenience, so that in Eq. (6) primary vaccination only moves individuals from the fully susceptible class to the recently vaccinated class. Eq. (7) reflects the fact that the immunity of naive individuals cannot wane.

2.2. Ordinary differential equation model

To make system (2)-(4) more tractable, we discretize the partial differential equations. Discretization requires us to assume proportionate mixing (i.e., contacts of a person aged a are distributed over those of all ages including their own in proportion to the contacts (i.e., products of *per capita* contact rates and numbers) of members of those age groups (Hethcote, 2000)). We assume that there are N such groups in the population defined by age intervals $[a_{n-1}, a_n)$, where $0=a_0<a_1<\ldots<a_{N-1}<a_N=\infty$, and that each group has aging rate τ_n, death rate $\mu(a)=\mu_n$, and fertility rate $f(a)=f_n$. Additionally, we assume that the transfer rates between susceptible and infected classes are given by α_{in}, ω_{in}, ρ_{in}, β_{jm}, and γ_{jm}, where $i(j)$ and $n(m)$ denote the immunity status and age group of the $S(I)$ classes, respectively. Parameter definitions are given in Table 2. The discretization is outlined in Appendix A and follows the steps described in Hethcote (2000). The ODE system is as follows:

$$\begin{aligned}
S'_{11} &= \sum_{j=1}^{5}\sum_{m=1}^{N} f_m T_{jm} - \tau_1 S_{11} - \Lambda_{11}S_{11} - \mu_1 S_{11} + \omega_{21}S_{21} - \rho_{11}S_{11},\\
S'_{21} &= -\tau_1 S_{21} - \Lambda_{21}S_{21} - \mu_1 S_{21} + \omega_{31}S_{31} - \omega_{21}S_{21} - \rho_{21}S_{21},\\
S'_{31} &= -\tau_1 S_{31} - \Lambda_{31}S_{31} - \mu_1 S_{31} + \omega_{41}S_{41} - \omega_{31}S_{31} - \rho_{31}S_{31},\\
S'_{41} &= -\tau_1 S_{41} - \Lambda_{41}S_{41} - \mu_1 S_{41} + \omega_{51}S_{51} - \omega_{41}S_{41}\\
&\quad + \rho_{11}S_{11} - \rho_{41}S_{41},\\
S'_{51} &= -\tau_1 S_{51} - \mu_1 S_{51} - w_{51}S_{51} + \sum_{j=1}^{4}\gamma_{j1}I_{j1} + \sum_{j=2}^{4}\rho_{j1}S_{j1},\\
S'_{in} &= \tau_{n-1}S_{i(n-1)} - \tau_n S_{in} - \Lambda_{in}S_{in} - \mu_n S_{in}\\
&\quad + \omega_{i+1,n}S_{i+1,n} - \omega_{in}S_{in} + \psi_i\rho_{1n}S_{1n} - \rho_{in}S_{in},\\
S'_{5n} &= \tau_{n-1}S_{5(n-1)} - \tau_n S_{5n} - \mu_n S_{5n} - w_{5n}S_{5n}\\
&\quad + \sum_{j=1}^{4}\gamma_{jn}I_{jn} + \sum_{j=2}^{4}\rho_{jn}S_{jn},\\
I'_{i1} &= -\tau_1 I_{i1} + \Lambda_{i1}S_{i1} - \mu_1 I_{i1} - \gamma_{i1}I_{i1},\\
I'_{in} &= \tau_{n-1}I_{i(n-1)} - \tau_n I_{in} + \Lambda_{in}S_{in} - \mu_n I_{in} - \gamma_{in}I_{in},\\
&\quad 1\le i\le 4, 2\le n\le N
\end{aligned} \tag{8}$$

where, $\tau_N=0$, and $\Lambda_{ik}(t)=\alpha_{ik}A_k\lambda_{ik}(t)$, with

$$\lambda_{ik}(t)=\frac{\sum_{j=1}^{4}\sum_{m=1}^{N}A_m\beta_{jm}I_{jm}(t)}{\sum_{m=1}^{N}A_m P_m}, \quad 1\le i\le 5,\ 1\le k\le N.$$

A derivation of the expression for $\lambda_{ik}(t)$ can be found in Appendix A.

The parameters used in system (8) are given in Table 2.

3. Analytical results

We begin by finding the steady states of our ODE model, system (8). Then we consider the stability of the disease-free equilibrium through calculation of the basic and control reproduction numbers, $\mathcal{R}_0$ and $\mathcal{R}_v$.

3.1. Steady states

Recall that the total population of age group i is given by $P_i=S_i+I_i$. Under our assumption of no disease-induced mortality, observe that

$$\begin{aligned}
\frac{dP_1}{dt} &= \sum_{m=1}^{N} f_m P_m - (\tau_1+\mu_1)P_1,\\
\frac{dP_n}{dt} &= \tau_{(n-1)}P_{(n-1)} - (\tau_n+\mu_n)P_n, \quad 2\le n\le N-1,\\
\frac{dP_N}{dt} &= \tau_{(N-1)}P_{(N-1)} - \mu_N P_N.
\end{aligned}$$

Following (Hethcote, 2000), we assume that

$$\sum_{m=1}^{N} f_m P_m = (\tau_1+\mu_1+q)\tilde{P}_1,$$

where $\tilde{P}_1$ is the size of the first age group at steady state. Then, given that $\tilde{P}_1$, P_1 are known, all P_m, $2\le m\le N$ can be solved. Under these conditions, the growth rate q can be solved using the following equation

$$\begin{aligned}
F(q) := &\frac{f_1}{\tau_1+\mu_1+q} + \frac{f_2\tau_1}{(\tau_2+\mu_2+q)(\tau_1+\mu_1+q)} + \cdots\\
&+ \frac{f_N\tau_{(N-1)}\tau_{(N-2)}\cdots\tau_2\tau_1}{\mu_N\big(\tau_{(N-1)}+\mu_{(N-1)}+q\big)\cdots(\tau_2+\mu_2+q)(\tau_1+\mu_1+q)}\\
&= 1.
\end{aligned} \tag{9}$$

In addition, the basic reproduction number of the population is given by

$$\mathcal{R}_{pop}=F(0).$$

Using this relationship, we find the disease-free equilibrium (DFE)

$$S^*_{1m}=P_m, \quad S^*_{2m}=S^*_{3m}=S^*_{4m}=S^*_{5m}=I^*_{1m}=I^*_{2m}=I^*_{3m}=I^*_{4m}=0, \quad 1\le m\le N,$$

Table 2
Parameter definitions for the PDE and ODE systems given in Eqs. (2)-(7) and Eq. (8), respectively, and notations used in Section 2. Subscripts i and j refer to immune status ($1 \le i \le 5$, $1 \le j \le 4$) and m and n refer to age groups. For simulations, we assume that several parameters are age-independent; i.e., $\alpha_{in} = \alpha_i$, $\omega_{in} = \omega_i$, $\beta_{jm} = \beta_j$, and $\gamma_{jm} = \gamma_j$. We also ignore disease-induced mortality; i.e., $\gamma_{jm} = 0$.

Parameter	Definition
f_n	fertility rate of individuals in age group n
μ_n	natural mortality rate of individuals in age group n
τ_n	aging rate of individuals in age group n
A_n	*per capita* contact rate of individuals in age group n
P_n	population size of age group n
$\tilde{P}_1$	population size of the first age group at stable age distribution
α_{in}	susceptibility of individuals from S_{in}
ω_{in}	rate of immunity waning of individuals from S_{in}
ρ_{in}	vaccination (primary and booster doses) rate of individuals from S_{in}
β_{jm}	infectivity of infected individuals from I_{jm}
γ_{jm}	recovery rate of infected individuals from I_{jm}
Notation	**Biological Interpretation**
$\Lambda_{in} = \alpha_{in} A_n \lambda$	force of infection for immune state i and age group n
$\Lambda_{in} S_{in}$	incidence for immune state i and age group n
$\sum_i \Lambda_{in} S_{in}$	incidence for age group n
$\sum_n \Lambda_{in} S_{in}$	incidence for immune state i
$\sum_i \sum_n \Lambda_{in} S_{in}$	incidence for immune state i and age group n
d_{jm}	average lifetime of an infected I_{jm} with immune status j and age m defined in Eq. (B.1)
π_{jm}	survival probability of an infectious individual in group (j, m) to next age group defined in Eq. (11)
$\tilde{T}_{jm}$	total population in group (j, m) at the DFE
q	growth rate of the total population at stable age distribution
$\mathcal{R}_{pop}$	population reproduction number
$\mathcal{R}_0$	basic reproduction number
$\mathcal{R}_v$	control reproduction number

where the total population of each age group m is denoted by P_m.

The endemic equilibrium is found by solving the linear system, $E_m s_m = v_m$, where $s_m = (S_{1m}, \ldots, S_{5m})^T$, $v_m = \tau_{(m-1)} s_{(m-1)} + (0, 0, 0, 0, \tilde{i}_{(m-1)})^T$, $\tilde{i}_{(m-1)} = \sum_{j=1}^{4} \left(\gamma_{jm} d_{jm} \tau_{(m-1)} I_{j(m-1)}\right)$, and the coefficient matrix is

$$E_m = \begin{pmatrix} r_{1m} & -\omega_{2m} & 0 & 0 & 0 \\ 0 & r_{2m} & -\omega_{3m} & 0 & 0 \\ 0 & 0 & r_{3m} & -\omega_{4m} & 0 \\ -\rho_{1m} & 0 & 0 & r_{41} & -\omega_{5m} \\ -\Gamma_{1m} & -\Gamma_{2m} - \rho_{2m} & -\Gamma_{3m} - \rho_{3m} & -\Gamma_{4m} - \rho_{4m} & r_{5m} \end{pmatrix},$$

with $\Gamma_{jm} = \gamma_{jm} d_{jm} \Lambda_{jm}$ for $1 \le j \le 4$ and $1 < m \le N$. Derivation of this linear system is found in Appendix B. Note that matrix E_m is column strictly diagonally dominant thus invertible, whereupon we can solve for $s_m = E_m^{-1} v_m$, where the elements of v_m are known from step $m-1$. By the method of mathematical induction, we then obtain the steady state solutions for system (8).

3.2. Reproduction numbers $\mathcal{R}_v$ and $\mathcal{R}_0$

We first consider the control reproduction number $\mathcal{R}_v$. Let $\tilde{T}_{jm}$ and $\tilde{P}_m$ denote the population sizes corresponding to T_{jm} and P_m, respectively, at the disease-free equilibrium. Now, let

$$\tilde{c}_{jm} = \frac{A_m \tilde{T}_{jm}}{\sum_{r=1}^{N} A_r \tilde{P}_r}, \tag{10}$$

$$\pi_{jm} = \tau_m d_{jm}, \tag{11}$$

where d_{jm}, the average sojourn of an infected individual I_{jm} with immune status j and age m, is given by Eq. (B.1), and π_{jm} is the survival probability of an infected individual from group (j, m) to the next age group $(m+1)$. Recall that

$$I_{j1} = d_{j1} \Lambda_{j1} S_{j1}, \quad I_{jm} = d_{jm} \Lambda_{jm} S_{jm} + d_{jm} \tau_{m-1} I_{j(m-1)}.$$

Then, iteratively, we find

$$I_{jm} = Q_{jm} \lambda, \tag{12}$$

where λ is defined in Eq. (A.4), and

$$\begin{aligned} Q_{jm} = {} & d_{jm} \alpha_{jm} A_m S_{jm} + d_{jm} \pi_{j(m-1)} \alpha_{j(m-1)} A_{m-1} S_{j(m-1)} \\ & + \ldots + d_{jm} \pi_{j(m-1)} \pi_{j(m-2)} \cdots \pi_{j(m-k)} \alpha_{j(m-k)} A_{m-k} S_{j(m-k)} \\ & + \cdots + d_{jm} \pi_{j(m-1)} \pi_{j(m-2)} \pi_{j(m-3)} \cdots \pi_{j1} \alpha_{j1} A_1 S_{j1}, \end{aligned}$$

giving

$$Q_{jm} = d_{jm} \sum_{k=1}^{m} \left(\prod_{s=k}^{m-1} \pi_{js} \right) \alpha_{jk} A_k S_{jk}. \tag{13}$$

Note that $\prod_{s=k}^{k-1} \pi_{js} = 1$. Now, substituting Eq. (12) into Eq. (A.4), we have

$$\lambda = \sum_{j=1}^{4} \frac{\sum_{m=1}^{N} A_m \beta_{jm} I_{jm}}{\sum_{j=1}^{5} \sum_{r=1}^{N} A_{jr} T_{jr}} = \sum_{j=1}^{4} \frac{\sum_{m=1}^{N} A_m \beta_{jm} Q_{jm} \lambda}{\sum_{j=1}^{5} \sum_{r=1}^{N} A_{jr} T_{jr}}.$$

Dividing by λ, we obtain

$$1 = \sum_{j=1}^{4} \frac{\sum_{m=1}^{N} A_m \beta_{jm} Q_{jm}}{\sum_{j=1}^{5} \sum_{r=1}^{N} A_{jr} T_{jr}}.$$

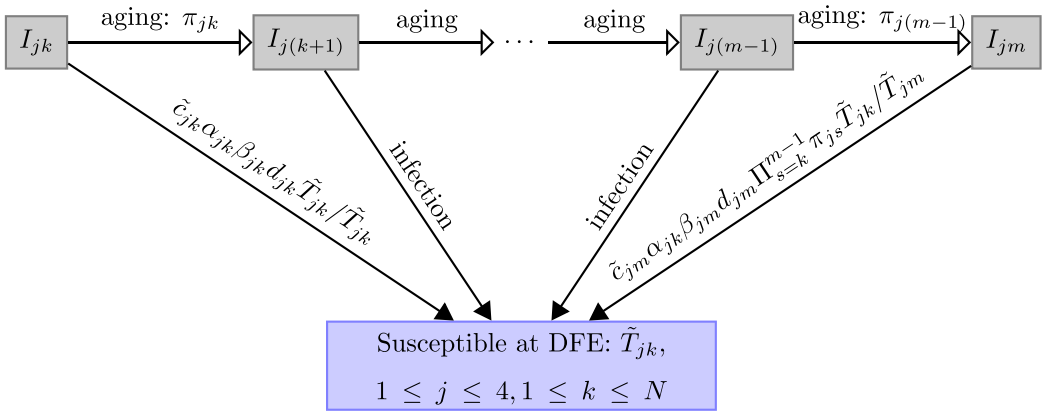

Fig. 2. Diagram showing the total number of secondary infections generated by an infectious person who became infected while in the (j, k) group. The horizontal progressions indicate that infectious people may age to the next group (infectious and alive) with probability π_{jk}.

Denoting by Q^0_{jm} what we get by substituting $\lambda = 0$ into Q_{jm} (meaning that the S compartments are at the disease-free equilibrium), we have

$$Q^0_{jm} = d_{jm}\sum_{k=1}^{m}\left(\prod_{s=k}^{m-1}\pi_{js}\right)\alpha_{jk}A_k\tilde{T}_{jk},$$

where $\tilde{T}_{jk}$ denotes the susceptible individuals at the DFE. Now we define

$$\begin{aligned}\mathcal{R}_v &= \sum_{j=1}^{4}\frac{\sum_{m=1}^{N}A_m\beta_{jm}Q^0_{jm}}{\sum_{j=1}^{5}\sum_{r=1}^{N}A_r\tilde{T}_{jr}}\\ &= \sum_{j=1}^{4}\sum_{m=1}^{N}\frac{\tilde{c}_{jm}}{\tilde{T}_{jm}}\beta_{jm}d_{jm}\sum_{k=1}^{m}\left(\prod_{s=k}^{m-1}\pi_{js}\right)\alpha_{jk}A_k\tilde{T}_{jk}\\ &= \sum_{j=1}^{4}\sum_{m=1}^{N}\sum_{k=1}^{m}\alpha_{jk}A_k\tilde{c}_{jm}\beta_{jm}d_{jm}\left(\prod_{s=k}^{m-1}\pi_{js}\right)\frac{\tilde{T}_{jk}}{\tilde{T}_{jm}}.\end{aligned} \tag{14}$$

Interchanging the latter two sums, the above equation leads to our expression for $\mathcal{R}_v$ in Theorem 1.

Theorem 1. *When proportionate mixing, given by (A.3), is used in system (8), the control reproduction number $\mathcal{R}_v$ (v for vaccination) is given by*

$$\mathcal{R}_v = \sum_{j=1}^{4}\sum_{k=1}^{N}\sum_{m=k}^{N}\alpha_{jk}A_k\tilde{c}_{jm}\beta_{jm}d_{jm}\left(\prod_{s=k}^{m-1}\pi_{js}\right)\frac{\tilde{T}_{jk}}{\tilde{T}_{jm}}. \tag{15}$$

The fraction $\tilde{T}_{jk}/\tilde{T}_{jm}$ can be interpreted according to the transmission term in the model. That is, $\tilde{T}_{jk}$ is the total number of susceptible individuals in group (j, k) at the disease-free equilibrium who are capable of being infected, and $1/\tilde{T}_{jm}$ is the probability that a contact is with the initially introduced infectious individual while in group (j, m).

Before we present the proof of Theorem 1, we provide a biological interpretation of the expression for $\mathcal{R}_v$ given in (15). A schematic diagram showing the total number of secondary infections generated by an infectious person who became infected while in group (j, k) is given in Fig. 2.

An infectious individual can infect susceptible individuals in any of the $4 \times N$ sub-groups, S_{jn} with immune status $1 \le j \le 4$ and age group $1 \le n \le N$. For susceptible individuals in each of these groups, their total contacts with all individuals in group (j, m) are $\tilde{c}_{jm}$. If an individual became infectious in group (j, k) with $k < m \le N$, the average time spent in this group would be d_{jm}. The probabilities of this individual aging (alive and infectious) to group $(j, k+1)$ is π_{jk} and group (j, m) are $\prod_{s=k}^{m-1}\pi_{js}$. Note that an infectious person in group (j, m) has infectivity β_{jm}. Now, the total number of susceptible individuals in group (j, k) at the DFE is $\tilde{T}_{jk}$, and the probability of any of the susceptible individuals in group (j, k) contacting this infectious individual in group (j, m) is $\tilde{c}_{jm}/\tilde{T}_{jm}$. Note also that α_{jk} denotes the susceptibility of individuals in group (j, k) and A_k is the *per capita* contact rate of individuals in age group k.

Thus, the number of new infections generated per susceptible individual in group (j, k) by the infected person while in group (j, m) is

$$\alpha_{jk}A_k\beta_{jm}d_{jm}\left(\prod_{s=k}^{m-1}\pi_{js}\right)\frac{\tilde{c}_{jm}}{\tilde{T}_{jm}}.$$

And, for an individual who became infectious in group (j, k), after aging and surviving into group (j, m) $(k \le m \le N)$ while still infectious, the total number of new infections that s/he could possibly generate from susceptible individuals in group (j, k) is

$$\alpha_{jk}A_k\tilde{c}_{jm}\beta_{jm}d_{jm}\left(\prod_{s=k}^{m-1}\pi_{js}\right)\frac{\tilde{T}_{jk}}{\tilde{T}_{jm}}.$$

Furthermore, the number of new infections generated from susceptible individuals in group (j, k) by this infectious individual during his/her infectious period is

$$\sum_{m=k}^{N}\alpha_{jk}\tilde{c}_{jm}\beta_{jm}d_{jm}\left(\prod_{s=k}^{m-1}\pi_{js}\right)\frac{\tilde{T}_{jk}}{\tilde{T}_{jm}}.$$

Therefore, for all susceptible individuals; *i.e.*, summation over all $1 \le j \le 4$ and $1 \le k \le N$, the total number of new infections is $\mathcal{R}_v$ as given in Eq. (15).

To prove Theorem 1, we adopt the approach of Hethcote (2000). That is, a possible formula for $\mathcal{R}_v$ can be obtained by deriving the threshold condition for the existence of an endemic equilibrium. This expression for $\mathcal{R}_v$ is then examined by considering the dominate eigenvalue of the next generation matrix, as well as its biological interpretation. See Appendix C for the proof of Theorem 1.

When no vaccination program is implemented; *i.e.*, $\rho_{in} = 0$ $(1 \le i \le 4,\ 1 \le n \le N)$, the control reproduction number $\mathcal{R}_v$ reduces to the basic reproduction number, $\mathcal{R}_0$, given by

$$\mathcal{R}_0 = \sum_{j=1}^{4}\sum_{k=1}^{N}\sum_{m=k}^{N}\alpha_{jk}A_k\tilde{c}_{jm}\beta_{jm}d_{jm}\left(\prod_{s=k}^{m-1}\pi_{js}\right)\frac{\tilde{T}^0_{jk}}{\tilde{T}^0_{jm}}$$

$$= \sum_{k=1}^{N}\sum_{m=k}^{N} \alpha_{1k}A_k\tilde{c}_{1m}\beta_{1m}d_{1m}\left(\prod_{s=k}^{m-1}\pi_{1s}\right)\frac{\tilde{T}^0_{1k}}{\tilde{T}^0_{1m}},$$

where $\tilde{T}^0_{jk} = 0$ for $1 < j \leq 4$ is the total number of susceptible individuals in group (j, k) when $\rho_{in} = 0$ $(1 \leq i \leq 4, 1 \leq n \leq N)$ because only immune class 1 is present at the DFE absent vaccination.

4. Numerical results

To examine the effects of waning and boosting of immunity to *B. pertussis* on the vaccination program in Sweden, we parameterized our model with observations on demographics Nations (2015), vaccine uptake and efficacy Gustafsson et al. (2006). We also relaxed the assumption of proportionate mixing used in deriving the ODE from PDE model and in deriving expressions for the reproduction number

4.1. Simulation methods and parameterization

Age distribution. Age is partitioned as follows: 0–19 years by single years, 20–44 years by 5-year groups, 45–74 years by 10-year groups, and 75 years and older (an open interval whose width we take to be 25 years). Overall, there are 29 age groups. The aging rate τ_i of age group i is

$$\tau_i = \frac{\mu_i + q}{e^{(\mu_i+q)w_i} - 1},$$

where μ_i is the natural mortality rate in age group i, q is rate of change of the total population, and w_i is the interval width for age group i Hethcote (2000). The natural mortality μ_i and natality f_i of age group i are computed from births, deaths, and population size by age for Sweden during 2014 Nations (2015). The rate of change of the total population q is determined by solving Eqn. (10) set equal to one. For Sweden, the rate of change of the total population (ignoring immigration) is $q = -3.15 \cdot 10^{-3}$ year^{-1}. See Table D.1 for the natality and mortality rates by age group and Fig. D.1 for the observed and calculated stable age distributions.

Contact rate and activity. For our simulations, we use the mixing matrix observed in a neighboring Nordic country. Parameter values for the contact matrix $c(a, \theta)$ were determined from Finnish participants in the PolyMod study Mossong et al. (2008) as follows: The contacts that each participant recorded on an average day were tabulated by participant and contact ages using the groups modeled. Then these contacts were divided by the numbers of participants in each age group to obtain average daily rates of contact per participant. Summed over all contact age groups (represented by columns of the contact matrix), these are the activities of each participant age group (represented by rows in the matrix). See Table D.1 for activities. Dividing the rates by their respective sums yields the proportions of the contacts that members of each age group have with members of all age groups including their own, $c(a)$. See Feng and Glasser (2018) for an example of these calculations.

Immunization. We determined the proportions immunized from the observed proportions vaccinated together with vaccine efficacy. We fitted gamma distributions to observed proportions vaccinated by age (Tiia Lepp, personal communication). We combined the doses that infants receive at 3, 5 and 12 months of age, to which we refer to as primary vaccination. Together with the expert opinion that this 3-dose series is 90% efficacious against mild disease (Patrick Olin, Birger Trollfors, personal communication), we estimate that 35% of infants and 55% of children aged 1 year were immunized against mild disease. Similarly, we estimate that the immunity of 11.1% of children aged 4 years, 62% of children aged 5 years, 17% of children aged 6 years, and 0.3% of children aged 7 years was boosted by re-vaccination. And that the immunity of 6.9% of children aged 13 years, 65% of children aged 14 years, 18% of children aged 15 years, and 0.1% of children aged 16 years was again boosted by re-vaccination.

The immunization rates (ρ) were calculated from the proportions immunized and time intervals during which immunization occurred. For the interval of a year, for example, the rate is

$$\rho = \frac{x(\tau + \mu)}{1 - x},$$

where

$$\Pr(\text{immunized}) = x = \frac{\rho}{\rho + \tau + \mu}.$$

See Table D.2 for percents immunized and immunization rates by age group.

Susceptibility and infectivity. We modeled susceptibility to infection as a linearly decreasing function of immune status, with those in the fully susceptible class, S_1, having the highest value ($\alpha_1 = 1$) and those in the completely immune class, S_5, not being susceptible ($\alpha_5 = 0$). Similarly, the infectivity of infectious classes decreases with increasing status such that $\mathcal{R}_0 = 13.6$ assuming proportionate mixing. See Table D.3 for status-specific parameter values.

Recovery and waning immunity. The recovery rate is determined as the reciprocal of the average infectious period. Individuals having some level of immunity by virtue of prior infection or vaccination (i.e., those in $I_2 - I_4$) have shortened infectious periods. Individuals in the completely immune class S_5 also lose their immunity more slowly than those in other immunity classes. See Table D.3 for the recovery rate and rates of waning immunity by immune status.

4.2. Simulation protocol

All simulations were performed in Matlab 2016a. Initial population sizes of each age group were set to the stable-age distribution. While the numbers in each group change over time (the Swedish population would be shrinking absent immigration), the proportions remain fixed absent disease-induced mortality. Accordingly, we present some results as proportions rather than absolute numbers. Simulations without vaccination begin with a single infectious individual in the most infectious state (I_1). After 100,000 days (~ 275 years), oscillations have damped. Vaccination is introduced to the population with endemic disease; i.e., initial conditions for the introduction of vaccination are the proportion in each age and immune status after 100,000 days without vaccination. After another 100,000 days, a first booster dose is introduced to the population with on-going primary vaccination; i.e., initial conditions for the introduction of the first booster dose are the proportion in each age and immune status after 100,000 days with vaccination. After another 100,000 days, a second booster dose is introduced to the population with on-going primary and booster vaccination of young children; i.e., initial conditions for the introduction of the second booster dose are the proportion in each age and immune status after 100,000 days with primary vaccination and first booster dose. Note that 100,000 days was chosen to ensure that the system reached equilibrium before a new intervention (e.g., primary vaccination, first booster dose, second booster dose) is introduced.

4.3. Simulation results

Natural infection occurs early in life. Absent vaccination, most children experience infection by 5 years of age, and nearly all by 10 years (Figs. D.2 and D.3, A1-B1). Above 6 years of age, less than 10% of each group is fully susceptible (i.e., in S_1), and by age 10 years, all proportions are less than 2%. Beyond 12 years of age, the proportion fully susceptible slowly increases as immunity acquired

by virtue of childhood infection wanes. Beyond 20 years, the proportion exceeds 10% (not shown).

Vaccination substantially reduces incidence. Primary vaccination greatly reduces incidence (Fig. 3, blue line). Despite increased incidence among 4–12 year-olds, the reduced incidence below age four and above age 12 compensates, reducing incidence in the population overall. Each booster dose further reduces incidence (Fig. 3, red and yellow lines), particularly in groups just above their recommended ages. Both boosters also reduce incidence among younger and older people because individuals who otherwise would have infected them have been immunized. Despite the incorporation of two booster doses in addition to primary vaccination, incidence in the four and five-year-olds remains elevated compared to pre-vaccination (Fig. D.4). However, this increase is primarily in the classes with mild or asymptomatic disease.

Primary vaccination significantly decreases the proportion of the population that is fully susceptible. The inclusion of a primary vaccination series, 2 doses during the first year of life, and third at 1 year (i.e., completed early during the second year), substantially decreases the proportion of children ($<$ 10 years) that are fully susceptible; i.e., in S_1 (Fig. 4, A1, red line), and upon infection most infectious; i.e., in I_1 (Fig. 4, B1, red line). This decrease in the fully susceptible class is mirrored by an increase in vaccine-induced immunity; i.e., S_4 (Fig. 4, A1, pale blue line). However, as vaccination replaces natural infection, the proportion of individuals in the completely immune class decreases markedly; i.e., S_5 (Fig. 4, A1, dark blue line). This decline is largest for young children (4–6 years), but persists even among older ages, and results in increases in infectious classes whose members experience immunity-moderated symptoms, and concomitantly decreased infectivity (i.e., $I_2 - I_4$), among children ($<$ 10 years) (Fig. 4, B). Despite a decline in the completely immune class S_5, the increase in vaccine-induced and other partially immune classes (i.e., $S_2 - S_4$) more than compensates, reducing the overall incidence of disease, as measured by ΛS_{ik} (Fig. 3). Primary vaccination reduces the number of infectious individuals in the population by 1.6%.

A booster dose among young children increases immunity among adolescents and results in mostly asymptomatic infections. When a first booster dose among young children (4–8 years) is included, nearly the entire population above age 5 is in the fully or one of the partially immune states (i.e., $S_2 - S_5$). The majority of children receive this booster dose at 5–6 years (Fig. D.3, A3). It substantially increases the proportion of older children in the completely immune class (i.e., S_5) compared with primary vaccination alone (Fig. 4, A2, dark blue line), and shifts the burden of infections largely to the asymptomatic class I_4 (Fig. 4, B2). Below 4 and above 15 years of age, the proportion in the fully immune class is less than that with primary vaccination alone (Fig. 4, B2). Nonetheless, this booster further reduces incidence relative to primary vaccination alone (Fig. 3, red line) and leads to an additional 8.1% reduction in the total number of infections (Fig. D.5). Although the reduction is negligible above age 25 years (Fig. 3), it is apparent for the youngest age groups ($<$ 5 years).

A second booster dose among adolescents increases their immunity and that of young adults, and results in more asymptomatic infections. The inclusion of a second booster dose among adolescents (13–16 years), along with primary vaccination and a booster dose among younger children, increases the proportion of the population in the fully immune class (i.e., S_5) through age 25 compared to primary vaccination plus a single booster (Fig. 4, A3). This booster also leads to a strong relative increase in the proportion of infections that are asymptomatic (and not infectious), particularly among ages 15–25 years. Similar to a single booster dose compared to primary vaccination alone, this increase in the proportion of individuals in S_5 at intermediate ages results in a decrease in those who are completely immune at younger ($<$ 12 years) and older ($>$ 25 years) ages (Fig. 4, A3). Also apparent is a slight relative increase in the most infectious class I_1 among children ages 2–12 years (Fig. 4, B3). In all age groups, despite changes in the proportion completely immune, incidence is reduced relative to primary vaccination alone. Comparing the second booster to the first, the reduction in incidence (Fig. 3) is most apparent among individuals aged 14–25 years, but also among young children ($<$ 6 years), and there is a further 6.7% reduction in the total infectious population.

Ages of booster doses correspond with waning of immunity. The timing and efficacy of primary vaccination and booster doses were estimated from Swedish observations (described in Section 4.1). Decisions about the ages at which booster doses should be introduced were based on preschool data from enhanced pertussis surveillance Gustafsson et al. (2006), nationwide data on anti-diphtheria immunity in children, and what at the time was believed the optimal dosing interval for diphtheria/tetanus boosters. The rate of immunity decay following infection or vaccination, which our model does not distinguish, was determined independently from a cross-sectional serological survey Feng et al. (2015), longitudinal studies Teunis et al., 2002, 2016, and clinical trials Olin et al., 1997.

Following primary vaccination alone, simulations indicate a marked decline in the partially immune classes at 5 years of age (Fig. 4, A1). Examination of all infections with and without primary vaccination (Fig. 5, C, crossing of blue and red lines) suggests an increase around 5 years of age following primary vaccination. If only infections with severe symptoms were observable, the increase might not be apparent until around 7 years of age (Fig. 5, A, crossing of blue and red lines). To prevent this observed increase, a booster dose in slightly younger age groups, such as starting at four years, might be recommended.

Note that simulations indicate a switch from an increase in the completely immune class to a decrease at approximately age 15 years following implementation of the first booster dose (Fig. 4, A2, dark blue line). This can also be seen in Fig. 5, C. To prevent this, a second booster dose in slightly younger age groups, such as starting at thirteen years, might be recommended.

Proportionate mixing enhances the apparent effectiveness of vaccination. While we assumed that mixing was proportionate to derive analytical expressions for the reproduction numbers, we used the mixing actually observed in Finland for our simulations. Had we assumed proportionate mixing, the burden of infection in younger age groups would have been greater (Fig. D.5). This affects the apparent impact of vaccination, making it seem more effective and its effect to last longer than with actual mixing. This can be seen by the age under which the infectious classes are larger with vaccination than without (Fig. D.6).

Reproduction numbers indicate that pertussis cannot be eliminated. Using the next generation matrix approach (van den Driessche and Watmough, 2002), we find these basic and control reproduction numbers: $\mathcal{R}_0 = 14.82$ and $\mathcal{R}_v = 12.41$, 10.01, and 8.45 with primary vaccination alone, primary plus the first booster, and primary plus both boosters, respectively. Note that nonrandom mixing increases reproduction numbers Feng et al. (2015), so this estimate of $\mathcal{R}_0$ is greater than that assuming proportionate mixing, which for the same parameter values is $\mathcal{R}_0 = 13.6$.

5. Discussion

Following vaccination or recovery from infection, hosts may be immune. Such immunity may be temporary or lifelong, and vaccine-induced immunity may differ from that acquired naturally, e.g., not last as long. If immunity decays, as it does against most bacterial and some viral pathogens, it may be boosted by exposure to infectious hosts or re-vaccination. Several vaccine doses may be needed to prevent disease following exposure to infectious hosts,

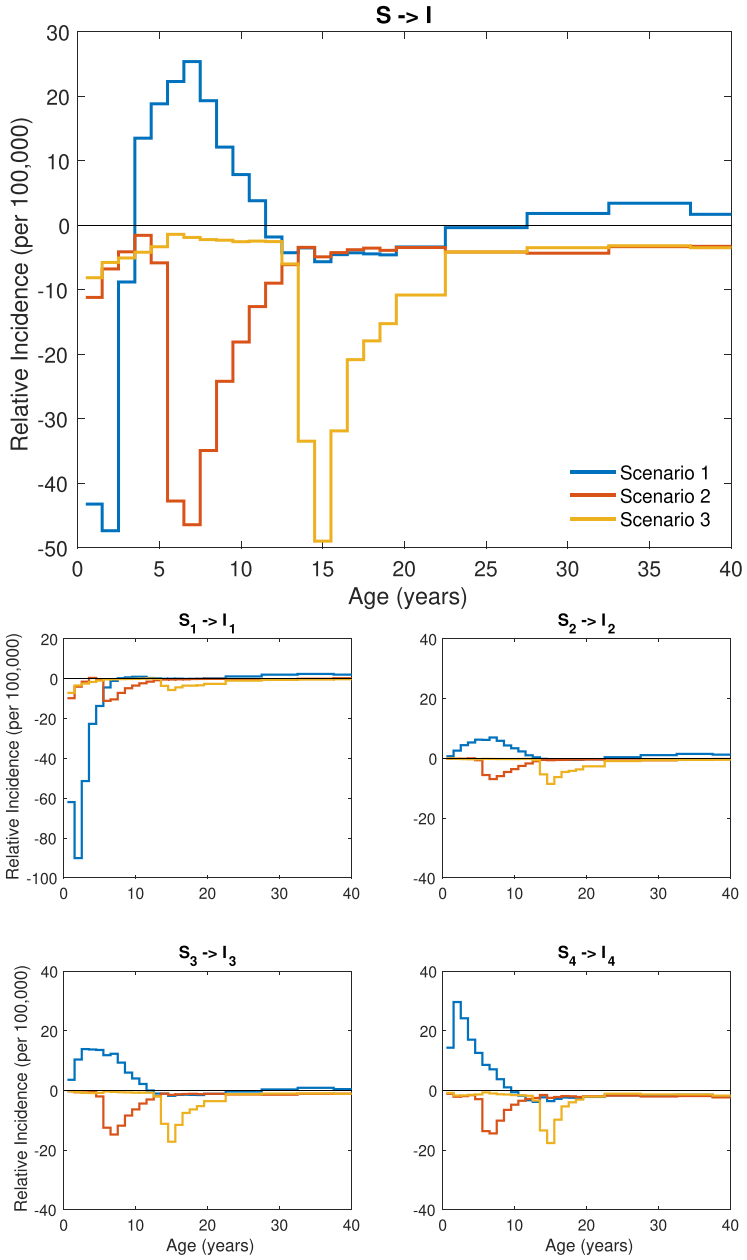

Fig. 3. Relative change in incidence by age. Comparisons of incidence by age group under different vaccination strategies: Scenario 1 - primary relative to no vaccination (blue); Scenario 2 - primary vaccination plus a single booster dose relative to primary vaccination alone (red); and Scenario 3 - primary vaccination plus two booster doses relative to primary vaccination with one (orange). The large panel is a composite of the smaller ones, which are for individual S classes. Negative values on the y-axes indicate that vaccination strategies reduce incidence. (For interpretation of the references to colour in this figure legend, the reader is referred to the web version of this article.)

i.e., to achieve full or sterilizing immunity. The severity of clinical symptoms that infected hosts experience may depend on their immune status when exposed, a function of time since recovery, vaccination, or most recent exposure, as well as infectious dose. And their infectiousness may depend on symptoms (e.g., coughing for pathogens transmitted via aerosols) as well as the intensity and duration of contact.

To design effective vaccination programs against the pathogens causing such diseases, one must appreciate how the prevalence of clinical disease – the tip of a proverbial iceberg, especially when surveillance is based on laboratory-confirmed infections – results from relations between host immunity, symptoms and infectivity. Such an understanding is also needed to appreciate the impact of vaccination, which changes the epidemiology of disease. Consequently, vaccination programs must be dynamic. In such situations, accurate transmission modeling can be invaluable. We devised a model that is faithful to the processes by which immunity waxes and wanes. Our model population is stratified by age largely because transmission is age-dependent, as consequently are vaccination schedules. As a proof-of-principle application, we attempt to reproduce the Swedish experience with pertussis.

The history of pertussis in Sweden offers a unique opportunity to explore the evolution of a vaccination program. Owing to universal healthcare, vaccination rates were high historically. However, in 1979, decreased efficacy of the whole-cell vaccine, together with some concerns about safety, led to the withdrawal of pertussis from the childhood vaccination schedule Romanus et al., 1987. In 1996, following clinical trials of several acellular candidates, vac-

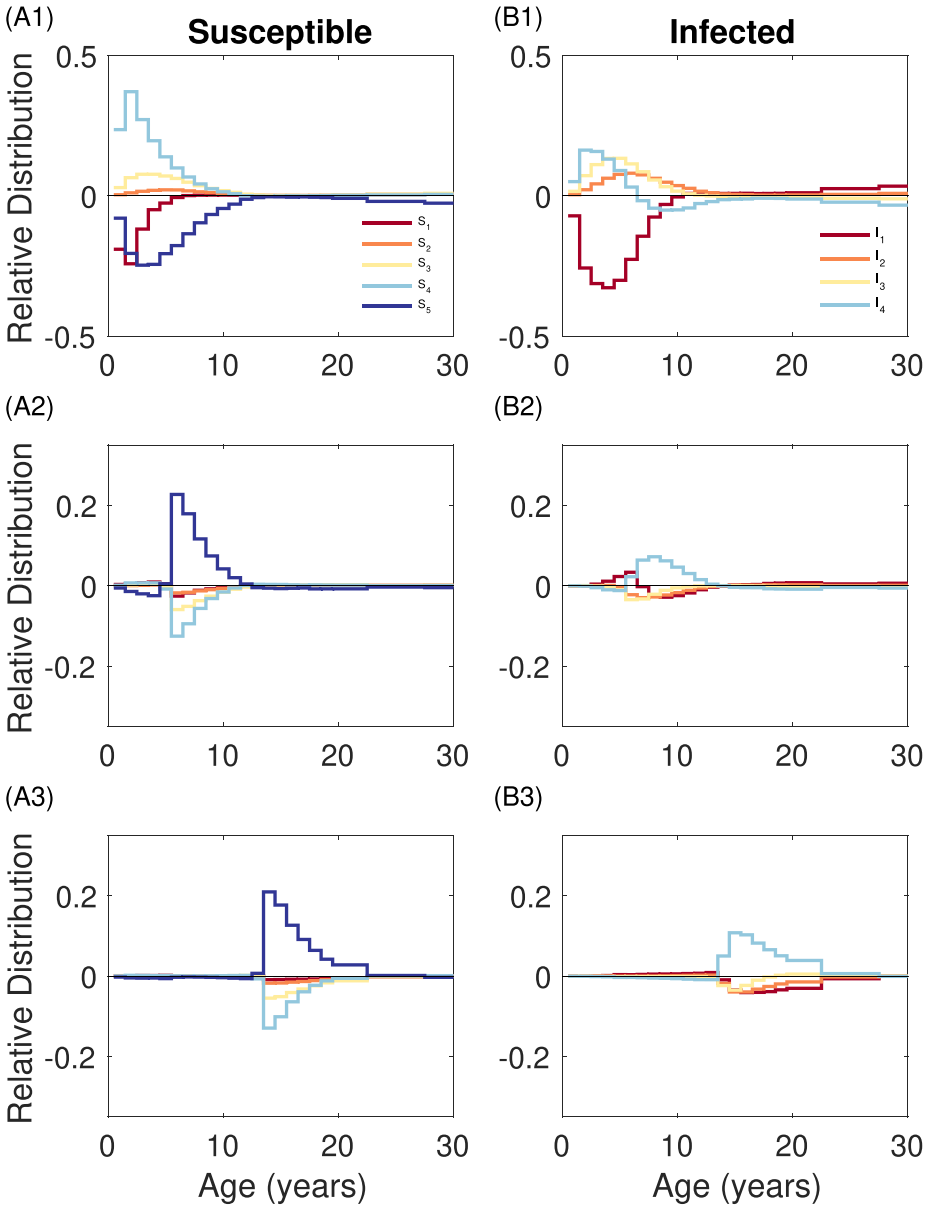

Fig. 4. Proportion of individuals shift between statuses. The relative change in proportion, normalized within age groups, is shown for (A) fully susceptible S_1 (red), low immunity S_2 (orange), medium immunity S_3 (yellow), vaccinated S_4 (light blue), and completely immune S_5 (blue) and for (B) severe symptoms and full infectivity I_1 (red), moderate symptoms and infectivity I_2 (orange), mild symptoms and low infectivity I_3 (yellow), and neither symptoms nor infectivity I_4 (light blue). (A1)-(B1) shows the difference between primary vaccination and no vaccination (Scenario 1 from Fig. 3). (A2)-(B2) shows the difference between primary vaccination with a single booster dose and primary vaccination alone (Scenario 2 from Fig. 3). (A3)-(B3) shows the difference between primary vaccination with both booster doses compared to primary vaccination with a single booster dose (Scenario 3 from Fig. 3). Colors from Brewer (2013). (For interpretation of the references to colour in this figure legend, the reader is referred to the web version of this article.)

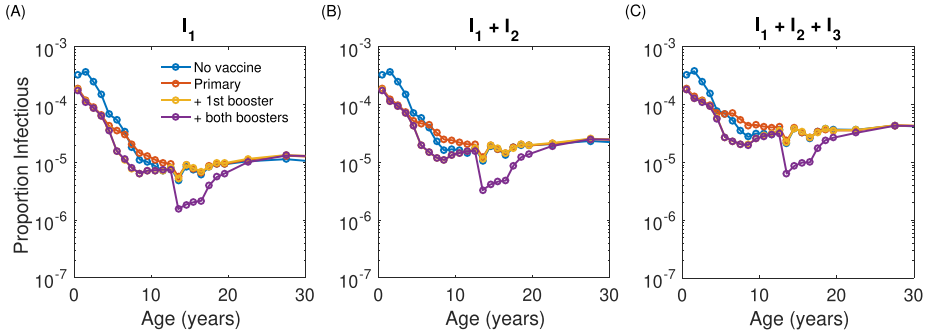

Fig. 5. Infectious population by symptomatic class. The proportion of infectious individuals with severe symptoms (A), severe and moderate symptoms (B) or any symptoms (C) under no vaccination (blue), primary vaccination alone (red), primary vaccination with the first booster dose (yellow) and primary vaccination with both booster doses (purple). Note that the y-axis is log scale. (For interpretation of the references to colour in this figure legend, the reader is referred to the web version of this article.)

cination was resumed Olin et al. (2003). Consequently, the experience of a 17-year cohort informs understanding of infection and the waning of natural immunity. Changes in incidence on resumption of vaccination further inform understanding of patterns invariably observed, but not necessarily as clearly as in Sweden, whenever pertussis is included in national vaccination programs.

Compared with most earlier pertussis models, ours includes fewer states (Fig. 1). Between fully susceptible and immune, we distinguish only three, the highest of which (S_4) is attained on completion of the primary vaccine series. If infected or re-vaccinated, hosts become completely immune. Immune state when infected determines host symptoms, which range from typically severe through moderate and mild to none. Generally, hosts seek medical care for typical and, to a lesser extent moderate disease. And laboratory confirmation is rarely sought, even among the youngest hosts for whom it could have therapeutic value (presumptive treatment is recommended in Sweden). Insofar as those with moderate and mild symptoms are nonetheless infectious, transmission and disease are largely occult. Infants, for whom pertussis may be fatal, especially during their first six months, are of special concern, as they may may have sufficiently intimate and prolonged contacts with mildly symptomatic caregivers for infection.

We formulate our model of waning and boosting as a system of partial differential equations (PDEs) with discrete immunity classes, but continuous age and time. Because most information is available for age ranges, we use the same approach as in Hethcote (2000) to convert it into a system of ordinary differential equations (ODEs) with 29 age classes. This requires the above-mentioned assumption of proportionate mixing that we relax in subsequent simulations performed to evaluate the impact of vaccination. We derive the reproduction numbers and determine the existence and characteristics of the disease-free and endemic equilibria. We provide intuitive explanations of model terms and all analytical results. Table 2, for one example, provides biological interpretations of various functions. Fig. 2, for another, illustrates the average number of secondary infections due to a host who was infected while in immune state j and age group k.

We used other observations made in (e.g., age distributions of vaccination, which we have courtesy of Tiia Lepp, Public Health Agency of Sweden) or appropriate for Sweden (e.g., the contact rates and mixing matrices used in our analyses and simulations were derived from observations of Finnish participants in the POLYMOD study, which we have courtesy of John Edmunds, London School of Public Health and Tropical Medicine) for our simulations. Where observations were lacking, we used the opinions of Swedish subject-matter experts.

We compared primary vaccination to none, the first booster to primary vaccination alone, and the second booster to primary vaccination plus the first by simulation. We found that primary and re-vaccination shifted the age-distributions of immunity at steady-state (Fig. 4), despite always reducing the total incidence. The infant series reduced typical disease among pre-school children, but we observed more mild and moderate disease among elementary school children (Fig. 3). On simulating the booster administered from 4 to 7 years, we found much less immunity-modified disease among those children, but an increase among adolescents. Similarly, on simulating the booster administered from 14 to 17 years, we found a decrease in immunity-modified disease among members of this age group. Significantly, by virtue of the age-distribution of the force of infection Feng et al., 2014, the adolescent booster did not shift immunity-modified disease into the reproductive years.

To facilitate converting the PDE system with which we began into an ODE system and derive analytical expressions for the reproduction numbers, we assumed that the probability of contacting a member of any group is proportional to the product of their *per capita* contact rate and population. This assumption, called proportionate mixing, is random with respect to available contacts. But, as mentioned, we used the contact rates observed in a nearby Nordic country in our simulations. As heterogeneity and non-random mixing affect reproduction numbers Feng et al. (2015), we compared simulations with proportionate and actual mixing, in which there are preferential contacts between parents and children as well as among contemporaries Glasser et al., (2012). Because vaccination does not seem as effective or long lasting with preferential as proportional mixing, the resurgence of immunity-modified disease seems to depend to some extent on non-random mixing Rohani et al. (2010).

Of the several attempts to explain the changing epidemiology of pertussis that accompanies successful routine vaccination programs, that by Lavine et al. (2011) is by far the most compelling. To an otherwise conventional SIR model, they add an immune state between fully susceptible and recently recovered or vaccinated. Unlike others who have considered boosting, they argue – based on the sensitivity of primed B- and T-cells – that previously infected hosts are more likely to have their immunity boosted than naive ones are to be infected. In our model, which includes only two more immune states, immune status is a function of time since previous exposure (infection, vaccination or boosting), and we assume that susceptibility and infectiousness both vary inversely with immune state. The result is a much more general model suitable for diseases caused by pathogens against which immunity wanes.

Public health officials learn about typical and to some extent moderately severe pertussis, possibly only among some of those for whom laboratory confirmation has therapeutic value. (Additionally, samples must be collected properly and shipped correctly for accurate laboratory results.) With transmission models that are faithful to the mechanisms underlying observed phenomena, however, they could consider the complete burden of disease. As far as we can tell from our simulations, the number and ages of booster doses are correct given the unusually effective primary series in Sweden. The steady-state analyses reported here do not permit evaluation of the timing of booster introductions. But public health officials in Sweden and elsewhere could use our model to monitor the information in Fig. 5, introduce boosters as needed, and evaluate their impact.

While our estimates of the control reproduction numbers suggest that pertussis cannot be eliminated, vaccination has substantial impact. The infant series reduces infections the most. Conditional on it, the booster among young children has less impact. Similarly, the adolescent booster has even less. The infant series also mitigates the most severe disease, followed by successive boosters. However, insofar as the adolescent booster not only reduces circulation of *B. pertussis*, but ensures that young adults are immune, it may prevent mildly symptomatic caregivers from infecting infants with tragic consequences. Finally, with regard to other hypothesized causes of the apparent resurgence of pertussis, we note that – together with vaccination – the waning and boosting of immunity is sufficient. We cannot disprove alternatives, but no other mechanism is necessary. And parsimony is a virtue in science.

Acknowledgments

The authors acknowledge the generous support of the American Institute of Mathematics (AIM) via workshop and SQuaRE grants. ZF acknowledges support from the National Science Foundation (NSF) via DMS-1814545 and the IR/D program. JMH acknowledges support from the Natural Sciences and Engineering Research Council of Canada (NSERC) and the York University Research Chair Pro-

gram. The authors thank Patrick Olin and Birger Trollfors for helpful discussions about pertussis and Tiia Lepp for observations from enhanced pertussis surveillance in Sweden. The authors also thank John Edmunds for permitting them to use observations from the PolyMod study.

Appendix A. Discretization

We first consider the mixing function. The assumption of proportionate mixing allows us to express $c(a, \theta)$ as

$$c(a,\theta) = \frac{A(\theta)\sum_{j=1}^{5} T_j(\theta,t)}{\int_0^\infty A(\theta)\sum_{j=1}^{5} T_j(\theta,t)d\theta}, \tag{A.1}$$

where $T_j(\theta, t)$ is the total population of individuals of age θ and immune status j at time t. We assume that the population has already reached its stable age distribution, *i.e.*, $T_i(a,t) = T_i(a)e^{-qt}$, where q is a measure of the rate of change in the total population. Thus, there is no time dependence in the expression for contacts, $c(a, \theta)$. Thus, the proportion of the contacts between an individuals aged a and individuals aged θ and immune status j, given by Eq. 1, is

$$c_j(a,\theta,t) = \frac{T_j(\theta,t)}{\sum_{j=1}^{5} T_j(\theta,t)} c(a,\theta) = \frac{A(\theta)T_j(\theta,t)}{\int_0^\infty A(\theta)\sum_{j=1}^{5} T_j(\theta,t)d\theta}.$$

This leads to the right hand side of Eq. (5) and first term on the right hand side of Eqs. (2) and (4),

$$\begin{aligned}
&\int_0^\infty \frac{c_j(a,\theta,t)\beta_j(\theta)I_j(\theta,t)}{T_j(\theta,t)}d\theta \\
&= \int_0^\infty \frac{\dfrac{A(\theta)T_j(\theta,t)}{\int_0^\infty A(\hat\theta)\sum_{j=1}^{5} T_j(\hat\theta,t)d\hat\theta}\beta_j(\theta)I_j(\theta,t)}{T_j(\theta,t)}d\theta \\
&= \frac{\int_0^\infty A(\theta)\beta_j(\theta)I_j(\theta,t)d\theta}{\int_0^\infty A(\hat\theta)\sum_{j=1}^{5} T_j(\hat\theta,t)d\hat\theta},
\end{aligned}$$

where $1 \le j \le 5$ Thus, to discretize to N age groups, we have

$$\begin{aligned}
\int_0^\infty \frac{c_j(a,\theta,t)\beta_j(\theta)I_j(\theta,t)}{T_j(\theta,t)}d\theta &= \frac{\int_0^\infty A(\theta)\beta_j(\theta)I_j(\theta,t)d\theta}{\int_0^\infty A(\hat\theta)\sum_{j=1}^{5} T_j(\hat\theta,t)d\hat\theta} \\
&= \frac{\sum_{m=1}^{N} A_m\beta_{jm}I_{jm}}{\sum_{m=1}^{N} A_m\sum_{j=1}^{5} T_{jm}},
\end{aligned}$$

where $1 \le m \le N$ refers to age group m (*e.g.*, T_{12} denotes the total population size in the first immune status (naive) and second age group). Let P_m denote the population size of age group m (regardless of immune status),

$$P_m = \sum_{j=1}^{5} T_{jm}, \quad T_{jm} = S_{jm} + I_{jm}, \quad 1 \le j \le 5, \quad 1 \le m \le N.$$

Then, we obtain the corresponding expression for $\lambda(a)$ in the discrete case:

$$\lambda_{ik}(t) = \sum_{j=1}^{4} \frac{\sum_{m=1}^{N} A_m\beta_{jm}I_{jm}(t)}{\sum_{m=1}^{N} A_m\sum_{j=1}^{5} T_{jm}} = \frac{\sum_{j=1}^{4}\sum_{m=1}^{N} A_m\beta_{jm}I_{jm}(t)}{\sum_{m=1}^{N} A_mP_m}, \tag{A.2}$$

where i and k refer to immune status and age group, respectively. Note that λ_{ik} is time dependent as the I_{jm} are time dependent. Recall that proportionate mixing assumes that the proportion of contacts of susceptible people in group (i, k) with people in group (j, m), $c_{ik,jm}$, depends only on the fraction of contacts by group (j, m). That is,

$$c_{ik,jm} = \frac{T_{jm}}{\sum_{j=1}^{5} T_{jm}} \frac{A_m\sum_{j=1}^{5} T_{jm}}{\sum_{m}^{N}\sum_{j=1}^{5} T_{jm}} = \frac{A_mT_{jm}}{\sum_{m=1}^{N} A_mP_m}, \tag{A.3}$$

which corresponds to the expression of $c_j(a, \theta)$ in the discrete case because ages a and θ are now age groups k and m, respectively. Using the mixing function given in (A.3), we again obtain the same expression as in Eq. (A.2) for the corresponding expression for $\lambda(a)$ in the discrete case. Note from (A.2) that λ_{ik} is in fact independent of i and k. Also, $c_{ik,jm}$ is independent of i and k. For ease of notation, denote λ_{ik} by λ and $c_{ik,jm}$ by c_{jm}; i.e., let

$$\lambda(t) := \lambda_{ik}(t), \quad 1 \le i \le 5, \quad 1 \le k \le N \tag{A.4}$$

and

$$c_{jm} := c_{ik,jm}, \quad 1 \le i \le 5, \quad 1 \le k \le N.$$

Now, the incidence for group (i, k) is $\alpha_{ik}A_kS_{ik}\lambda = \Lambda_{ik}S_{ik}$ for all i and k, and

$$\Lambda_{ik}(t) = \alpha_{ik}A_k\lambda(t)$$

is the force of infection. Although λ is independent of age class and immune status, it is time dependent as it is a function of the infectious classes I, which change with time.

Appendix B. Endemic Equilibrium (derivation of linear system)

Before determining the endemic equilibrium, we introduce some notation for convenience. Let

$$B = \sum_{j=1}^{5}\sum_{n=1}^{N} f_nT_{jn} = (\tau_1 + \mu_1 + q)\tilde{P}_1$$

denote the total birth rate for the population, and

$$d_{jm} = \frac{1}{\tau_m + \mu_m + \gamma_{jm}} \tag{B.1}$$

denote the average lifetime of an infected individual I_{jm} with immune status j and age m, and let

$$r_{jm} = \Lambda_{jm} + \tau_m + \mu_m + \omega_{jm} + \rho_{jm},$$

with $\omega_{1m} = 0$, $\Lambda_{5m} = 0$, $\rho_{5m} = 0$, $1 \le m \le N$, and $\tau_N = 0$. Additionally, let

$$R_m = \sum_{j=1}^{4} \gamma_{jm}I_{jm}, \qquad 1 \le m \le N \tag{B.2}$$

where R_m can be interpreted as the sum of all individuals recovering at age m (who ultimately move to S_5 in Model (8)).

Seeking the steady states, we set the time derivatives zero. Then we have the following relations for the first age group of susceptible individuals:

$$B = r_{11}S_{11} - \omega_{21}S_{21},$$

$$
\begin{aligned}
0 &= r_{21}S_{21} - \omega_{31}S_{31},\\
0 &= r_{31}S_{31} - \omega_{41}S_{41},\\
0 &= r_{41}S_{41} - \omega_{51}S_{51} - \rho_{11}S_{11},\\
0 &= r_{51}S_{51} - \sum_{j=2}^{4}\rho_{j1}S_{j1} - R_1.
\end{aligned} \tag{B.3}
$$

Before solving for S in System (B.3), we first consider R_1. From the I equations in System (8), we have

$$I_{j1} = d_{j1}\Lambda_{j1}S_{j1}, \quad 1 \le j \le 4.$$

Thus, for $m = 1$ in Eq. (B.2),

$$R_1 = \sum_{j=1}^{4}\gamma_{j1}I_{j1} = \sum_{j=1}^{4}\gamma_{j1}d_{j1}\Lambda_{j1}S_{j1}. \tag{B.4}$$

Now, substituting Eq. (B.4) into System (B.3), we can rewrite the susceptible individuals in the first age group as the linear system $E_1 s_1 = v_1$, where $s_1 = (S_{11}, \ldots, S_{51})^T$, $v_1 = (B, 0, 0, 0, 0)^T$, and the coefficient matrix is

$$E_1 = \begin{pmatrix} r_{11} & -\omega_{21} & 0 & 0 & 0\\ 0 & r_{21} & -\omega_{31} & 0 & 0\\ 0 & 0 & r_{31} & -\omega_{41} & 0\\ -\rho_{11} & 0 & 0 & r_{41} & -\omega_{51}\\ -\Gamma_{11} & -\Gamma_{21}-\rho_{21} & -\Gamma_{31}-\rho_{31} & -\Gamma_{41}-\rho_{41} & r_{51} \end{pmatrix},$$

where $\Gamma_{j1} = \gamma_{j1}d_{j1}\Lambda_{j1}$ for $1 \le j \le 4$. Note that the matrix E_1 is column strictly diagonally dominant (because $d_{j1}\gamma_{j1} < 1$, $r_{j1} = \Lambda_{j1} + \tau_1 + \mu_1 + \omega_{j1} + \rho_{j1} > \Lambda_{j1}d_{j1}\gamma_{j1} + \omega_{j1} + \rho_{j1}$, for $1 \le j \le 4$), hence invertible, giving rise to the unique solution $s_1 = E_1^{-1}v_1$. Given s_1, using Eq. () it is possible to determine the infectious components of the first age group $i_1 = (I_{11}, \ldots, I_{41})^T$.

Now we consider the other age groups of susceptible individuals, $s_m = (S_{1m}, \ldots, S_{5m})^T$, $(1 < m \le N)$, and assume that

$$s_{(m-1)} = \left(S_{1(m-1)}, \ldots, S_{5(m-1)}\right)^T \quad \text{and}$$
$$i_{(m-1)} = \left(I_{1(m-1)}, \ldots, I_{4(m-1)}\right)^T$$

are already calculated. For the susceptible compartments in System (8), we have these steady-state equations,

$$
\begin{aligned}
\tau_{(m-1)}S_{1(m-1)} &= r_{1m}S_{1m} - \omega_{2m}S_{2m},\\
\tau_{(m-1)}S_{2(m-1)} &= r_{2m}S_{2m} - \omega_{3m}S_{3m},\\
\tau_{(m-1)}S_{3(m-1)} &= r_{3m}S_{3m} - \omega_{4m}S_{4m},\\
\tau_{(m-1)}S_{4(m-1)} &= r_{4m}S_{4m} - \omega_{5m}S_{5m} - \rho_{1m}S_{1m},\\
\tau_{(m-1)}S_{5(m-1)} &= r_{5m}S_{5m} - \sum_{j=2}^{4}\rho_{jm}S_{jm} - R_m.
\end{aligned}
$$

To specify R_m from the I-equation in System (8), we first have

$$I_{jm} = d_{jm}\left(\Lambda_{jm}S_{jm} + \tau_{(m-1)}I_{j(m-1)}\right),$$

and thus

$$R_m = \sum_{j=1}^{4}\gamma_{jm}I_{jm} = \sum_{j=1}^{4}\left(\gamma_{jm}d_{jm}\Lambda_{jm}S_{jm} + \gamma_{jm}d_{jm}\tau_{m-1}I_{j(m-1)}\right).$$

Appendix C. Definition of R_v

We use the next generation matrix method van den Driessche and Watmough, 2002 to prove that the definition for $\mathcal{R}_v$ (Eqn. (14)) is valid. We restrict ourselves to the sub-model of infected people, $[I_{jm}]^T$. We form two matrices, F and V, which determine new infections and transitions among infectious states, respectively. To form these matrices, we require the partial derivatives of the infected equations from System (8) evaluated at the DFE.

For $1 \le i \le 4$ and $1 \le n \le N$, differentiating λ in (A.4) with respect to I_{in}, we have

$$\frac{\partial\lambda}{\partial I_{in}} = \frac{\beta_{in}A_n\left(\sum_{m=1}^{N}\sum_{j=1}^{5}A_m(S_{jm}+I_{jm})\right) - \left(\sum_{m=1}^{N}\sum_{j=1}^{4}\beta_{jm}A_mI_{jm}\right)A_n}{\left(\sum_{m=1}^{N}\sum_{j=1}^{5}A_m(S_{jm}+I_{jm})\right)^2}.$$

Evaluating at the DFE, we further get

$$\left.\frac{\partial\lambda}{\partial I_{in}}\right|_{\text{DFE}} = \frac{\beta_{in}A_n}{\sum_{m=1}^{N}\sum_{j=1}^{5}A_m\tilde{T}_{jm}}.$$

Matrix F is an $4N \times 4N$ matrix whose row indices change coordinately with indices i and n for $1 \le i \le 4$ and $1 \le n \le N$ and whose column indices change coordinately with indices j and r for $1 \le j \le 4$ and $1 \le r \le N$. Its elements, denoted by $F_{in,jr}$, are as follows:

$$F_{in,jr} = \frac{\alpha_{in}A_n\tilde{T}_{in}\beta_{jr}A_r}{\sum_{m=1}^{N}\sum_{j=1}^{5}A_m\tilde{T}_{jm}} = \frac{\alpha_{in}A_n\tilde{T}_{in}\tilde{c}_{jr}\beta_{jr}}{\tilde{T}_{jr}},$$

where $\tilde{c}_{jr}$ is defined in Eq. (10). Then, matrix F is given by the following 4×4 block matrix,

$$F = \left(F_{i,j}\right), \quad \text{for} \quad 1 \le i, j \le 4,$$

where each block is an $N \times N$ matrix given as follows

$$F_{i,j} = \begin{pmatrix} F_{i1,j1} & F_{i1,j2} & \cdots & F_{i1,jN}\\ F_{i2,j1} & F_{i2,j2} & \cdots & F_{i2,jN}\\ \vdots & \vdots & \ddots & \vdots\\ F_{iN,j1} & F_{iN,j2} & \cdots & F_{iN,jN} \end{pmatrix}, \quad \text{for} \quad 1 \le i, j \le 4.$$

Matrix V is an $4N \times 4N$ matrix given as follows,

$$\begin{pmatrix} V_1 & 0 & 0 & 0\\ 0 & V_2 & 0 & 0\\ 0 & 0 & V_3 & 0\\ 0 & 0 & 0 & V_4 \end{pmatrix},$$

where V_i $(1 \le i \le 4)$ is $N \times N$ matrix and given as follows,

$$\begin{pmatrix} \frac{1}{d_{i1}} & 0 & \cdots & 0 & 0 & 0\\ -\tau_1 & \frac{1}{d_{i2}} & 0 & \cdots & 0 & 0\\ 0 & -\tau_3 & \frac{1}{d_{i3}} & 0 & \cdots & 0\\ \vdots & \ddots & \ddots & \ddots & \ddots & \vdots\\ 0 & \cdots & 0 & -\tau_{(N-2)} & \frac{1}{d_{i(N-1)}} & 0\\ 0 & \cdots & 0 & 0 & -\tau_{(N-1)} & \frac{1}{d_{iN}} \end{pmatrix}, \qquad 1 \le i \le 4.$$

Hence, matrix V is a lower diagonal matrix and diagonal dominant. This implies that matrix V^{-1} exists, and is as follows,

$$\begin{pmatrix} V_1^{-1} & 0 & 0 & 0\\ 0 & V_2^{-1} & 0 & 0\\ 0 & 0 & V_3^{-1} & 0\\ 0 & 0 & 0 & V_4^{-1} \end{pmatrix}.$$

Let a_{ij} be the (i, j) entry of V_1^{-1}. Then

$$a_{ij} = \begin{cases} 0, & i < j,\\ d_{1i}, & i = j,\\ d_{1i}\prod_{k=j}^{i-1}\tau_k d_{1k}, & j < i. \end{cases}$$

Matrix V_2^{-1}, V_3^{-1}, and V_4^{-1} can be expressed similarly with the only change being from 1 to 2, 3, and 4, respectively.

Note also that all columns of F are multiples of each other, which implies that $\text{rank}(F) = 1$. Using the result that, when A is an $m \times n$ matrix and B is an $n \times k$ matrix,

$$\text{rank}(AB) \leq \min(\text{rank}(A), \text{rank}(B)).$$

Then, for the next generation matrix FV^{-1}, we know that

$$\text{rank}(FV^{-1}) = 1.$$

Hence, the spectral radius of the next generation matrix FV^{-1} is given by the sum of diagonal elements of the $4N \times 4N$ next generation matrix. It is exactly R_v given in Eq. (15). This can be verified as follows.

For the first N rows of the next generation matrix, the diagonal elements are given by

$$\left(FV^{-1}\right)_{11} = \frac{\alpha_{11}A_1\tilde{T}_{11}}{\sum_{m=1}^{N}\sum_{j=1}^{5}A_m\tilde{T}_{jm}}\sum_{m=1}^{N}\beta_{1m}A_m d_{1m}\left(\prod_{k=1}^{m-1}\pi_{1k}\right),$$

$$\left(FV^{-1}\right)_{22} = \frac{\alpha_{12}A_2\tilde{T}_{12}}{\sum_{m=1}^{N}\sum_{j=1}^{5}A_m\tilde{T}_{jm}}\sum_{m=2}^{N}\beta_{1m}A_m d_{1m}\left(\prod_{k=2}^{m-1}\pi_{1k}\right),$$

$$\left(FV^{-1}\right)_{33} = \frac{\alpha_{13}A_3\tilde{T}_{13}}{\sum_{m=1}^{N}\sum_{j=1}^{5}A_m\tilde{T}_{jm}}\sum_{m=3}^{N}\beta_{1m}A_m d_{1m}\left(\prod_{k=3}^{m-1}\pi_{1k}\right),$$

$$\vdots \quad \vdots \quad \vdots$$

$$\left(FV^{-1}\right)_{(N-1)(N-1)} = \frac{\alpha_{1(N-1)}A_{(N-1)}\tilde{T}_{1(N-1)}}{\sum_{m=1}^{N}\sum_{j=1}^{5}A_m\tilde{T}_{jm}}\sum_{m=N-1}^{N}\beta_{1m}A_m d_{1m}\left(\prod_{k=N-1}^{m-1}\pi_{1k}\right),$$

$$\left(FV^{-1}\right)_{NN} = \frac{\alpha_{1N}A_N\tilde{T}_{1N}}{\sum_{m=1}^{N}\sum_{j=1}^{5}A_m\tilde{T}_{jm}}\beta_{1N}A_N d_{1N}.$$

Adding the above N equations leads to

$$\sum_{k=1}^{N}\frac{\alpha_{1k}A_k\tilde{T}_{1k}}{\sum_{m=1}^{N}\sum_{j=1}^{5}A_m\tilde{T}_{jm}}\sum_{m=k}^{N}\beta_{1m}A_m d_{1m}\left(\prod_{s=k}^{m-1}\pi_{1s}\right)$$
$$= \sum_{k=1}^{N}\sum_{m=k}^{N}\alpha_{1k}A_k\tilde{c}_{1m}\beta_{1m}d_{1m}\left(\prod_{s=k}^{m-1}\pi_{1s}\right)\frac{\tilde{T}_{1k}}{\tilde{T}_{1m}}.$$

Similarly, for the second, third, and fourth N rows of the next generation matrix, their sums are similar expressions with the only change being from sub-index 1 to 2, 3, and 4, respectively. The sum of these four sums is exactly the expression of $\mathcal{R}_v$ in Eq. (15).

Appendix D. Additional Tables and Figures

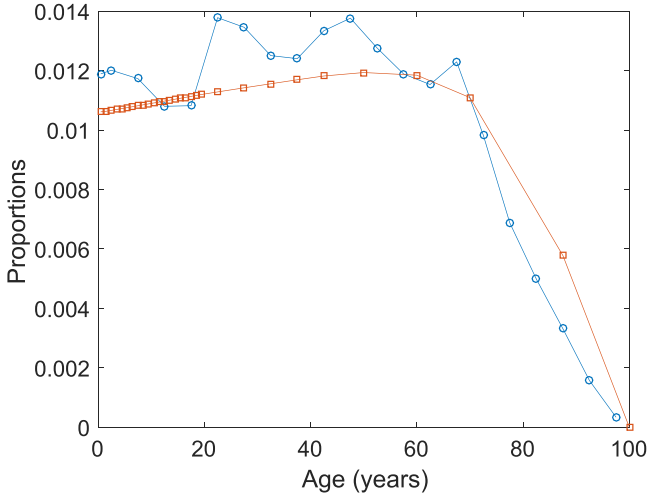

Fig. D.1. Population age distribution. The observed distribution (blue circles) is determined from information in Table D.1. The simulation age distribution is also shown (red squares). (For interpretation of the references to colour in this figure legend, the reader is referred to the web version of this article.)

Table D.1
Standard life-history parameters by age used for numerical simulations. The growth rate of the total population is calculated from the age-dependent parameters and found to be $q = -3.15 \cdot 10^{-3}$ year^{-1}.

Age group n	Age range (years)	Mortality rate μ_n (year^{-1})	Activity A_n (contacts · day^{-1})	Fecundity f_n (year^{-1})
1	0–1	$2.1160 \cdot 10^{-3}$	6.36	-
2	1-2	$2.7200 \cdot 10^{-5}$	8.37	-
3	2-3	$2.7200 \cdot 10^{-5}$	9.44	-
4	3–4	$2.7200 \cdot 10^{-5}$	9.39	-
5	4–5	$2.7200 \cdot 10^{-5}$	10.20	-
6	5–6	$1.4300 \cdot 10^{-5}$	10.27	-
7	6–7	$1.4300 \cdot 10^{-5}$	13.89	-
8	7–8	$1.4300 \cdot 10^{-5}$	14.77	-
9	8–9	$1.4300 \cdot 10^{-5}$	14.11	-
10	9–10	$1.4300 \cdot 10^{-5}$	15.38	-
11	10–11	$1.4100 \cdot 10^{-5}$	15.88	-
12	11–12	$1.4100 \cdot 10^{-5}$	17.81	-
13	12–13	$1.4100 \cdot 10^{-5}$	19.31	-
14	13–14	$1.4100 \cdot 10^{-5}$	10.71	-
15	14–15	$1.4100 \cdot 10^{-5}$	17.54	-
16	15–16	$4.9300 \cdot 10^{-5}$	14.35	$7.8453 \cdot 10^{-6}$
17	16–17	$4.9300 \cdot 10^{-5}$	11.40	$7.8453 \cdot 10^{-6}$
18	17–18	$4.9300 \cdot 10^{-5}$	12.14	$7.8453 \cdot 10^{-6}$
19	18–19	$4.9300 \cdot 10^{-5}$	13.31	$7.8453 \cdot 10^{-6}$
20	19–20	$4.9300 \cdot 10^{-5}$	11.62	$7.8453 \cdot 10^{-6}$
21	20–25	$4.4820 \cdot 10^{-4}$	9.16	$1.8044 \cdot 10^{-3}$
22	25–30	$4.7730 \cdot 10^{-4}$	11.15	$2.2112 \cdot 10^{-2}$
23	30–35	$6.1370 \cdot 10^{-4}$	10.60	$5.7899 \cdot 10^{-2}$
24	35–40	$5.6260 \cdot 10^{-4}$	13.98	$6.2700 \cdot 10^{-2}$
25	40–45	$9.1520 \cdot 10^{-4}$	11.87	$2.9840 \cdot 10^{-2}$
26	45–55	$1.9470 \cdot 10^{-3}$	11.10	$3.6000 \cdot 10^{-3}$
27	55–65	$5.3598 \cdot 10^{-3}$	8.48	$1.8500 \cdot 10^{-5}$
28	65–75	$1.3707 \cdot 10^{-2}$	6.18	-
29	75+	$7.5648 \cdot 10^{-2}$	2.67	-

Table D.2
Immunization by age. Here, the percent immunized is determined from the percent vaccinated and efficacy of the vaccine as described in the Section 4.1. Age groups that receive neither primary vaccination nor booster doses are omitted.

Age group n	Age range (years)	Percent immunized (% per year)	Immunization Rate ρ_n (year^{-1})	Application
1	0–1	34.98	0.5382	Primary vaccination
2	1–2	55.02	1.2250	Primary vaccination
3	2–3	0	0	-
4	3–4	0	0	-
5	4–5	11.06	0.1245	1st booster dose
6	5–6	62.01	1.6345	1st booster dose
7	6–7	16.61	0.1995	1st booster dose
8	7–8	0.29	0.0029	1st booster dose
9	8–9	0	0	-
10	9–10	0	0	-
11	10–11	0	0	-
12	11–12	0	0	-
13	12–13	6.93	0.0745	2nd booster dose
14	13–14	65.07	1.8658	2nd booster dose
15	14–15	17.88	0.2180	2nd booster dose
16	15–16	0.12	0.0012	2nd booster dose
17	16–17	0	0	-
18	17–18	0	0	-
19	18–19	0	0	-
20	19–20	0	0	-

Table D.3
Immune-status-dependent parameters used for numerical simulations. The subscript i refers to the immune status ranging from 1 (fully susceptible) to 5 (completely immune).

Immune status i	Susceptibility α_i	Infectivity β_i (day^{-1})	Immunity waning ω_i (year^{-1})	Recovery γ_i (day^{-1})
1	1.00	$8.67 \cdot 10^{-2}$	-	1/14
2	0.75	$8.28 \cdot 10^{-2}$	1/4	1/11
3	0.50	$7.59 \cdot 10^{-2}$	1/5	1/9
4	0.25	0.00	1/6	1/7
5	0.00	-	1/10	-

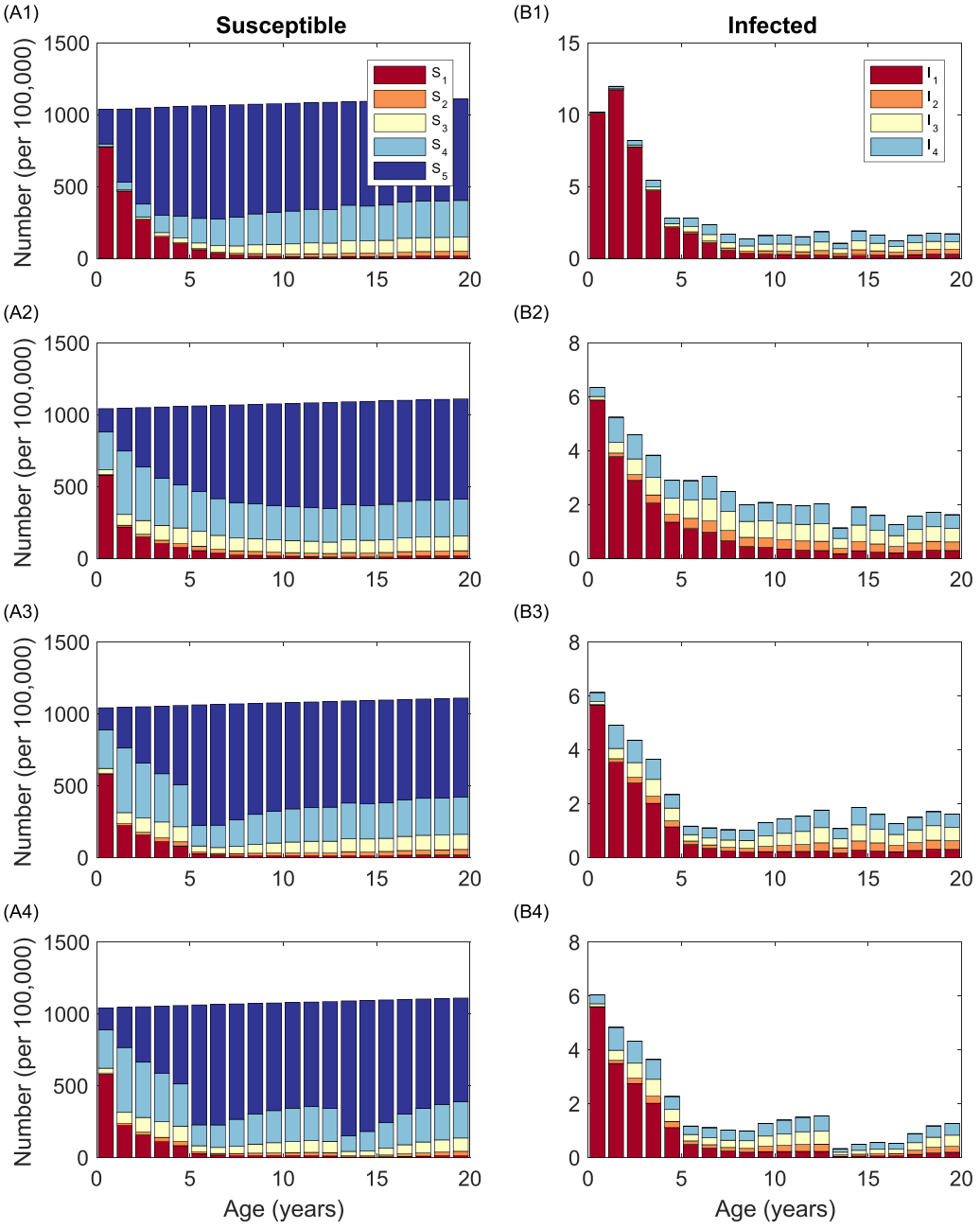

Fig. D.2. Distribution of individuals in each age class by immune status. The proportion of susceptible (A) or infected (B) individuals from the total population of each status with no vaccination (A1)-(B1), with primary vaccination alone (A2)-(B2), with primary vaccination plus one booster dose (A3)-(B3), with primary vaccination plus two booster doses (A4)-(B4). (Column (A)) Colors represent the level of susceptibility: fully susceptible S_1 (red), low partial immunity S_2 (orange), medium partial immunity S_3 (yellow), vaccinated immunity S_4 (light blue), and complete immunity S_5 (blue). (Column (B)) Colors represent the level of symptoms and transmissibility: severe symptoms and full transmissibility I_1 (red), moderate symptoms and transmissibility I_2 (orange), mild symptoms and low transmissibility I_3 (yellow), and neither symptoms nor transmissibility I_4 (light blue). The height of the bars in the top row indicates the total proportion in each age class while the bottom row is normalized by age group. Colors from Brewer (2013). (For interpretation of the references to colour in this figure legend, the reader is referred to the web version of this article.)

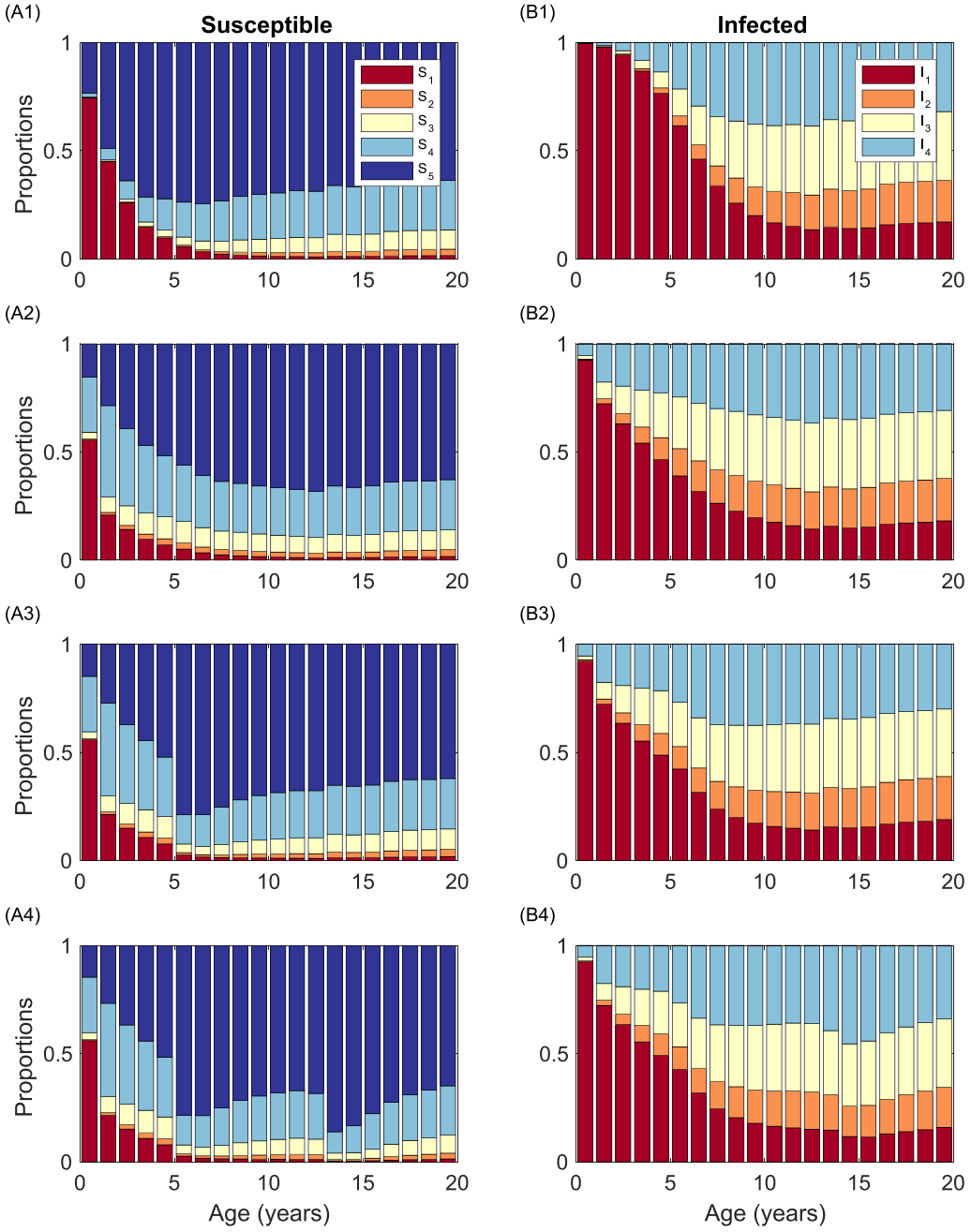

Fig. D.3. Distribution of individuals in each age class by immune status. The proportion of susceptible (A) or infected (B) individuals from the total population of each status with no vaccination (A1)-(B1), with primary vaccination only (A2)-(B2), with primary vaccination plus one booster dose (A3)-(B3), with primary vaccination plus two booster doses (A4)-(B4). (Column (A)) Colors represent the level of susceptibility: fully susceptible S_1 (red), low partial immunity S_2 (orange), medium partial immunity S_3 (yellow), vaccinated immunity S_4 (light blue), and complete immunity S_5 (blue). (Column (B)) Colors represent the level of symptoms and transmissibility: severe symptoms and full transmissibility I_1 (red), moderate symptoms and transmissibility I_2 (orange), mild symptoms and low transmissibility I_3 (yellow), and neither symptoms nor transmissibility I_4 (light blue). The height of the bars in the top row indicate the total proportion in each age class while the bottom row is normalized by age group. Colors from Brewer (2013). (For interpretation of the references to colour in this figure legend, the reader is referred to the web version of this article.)

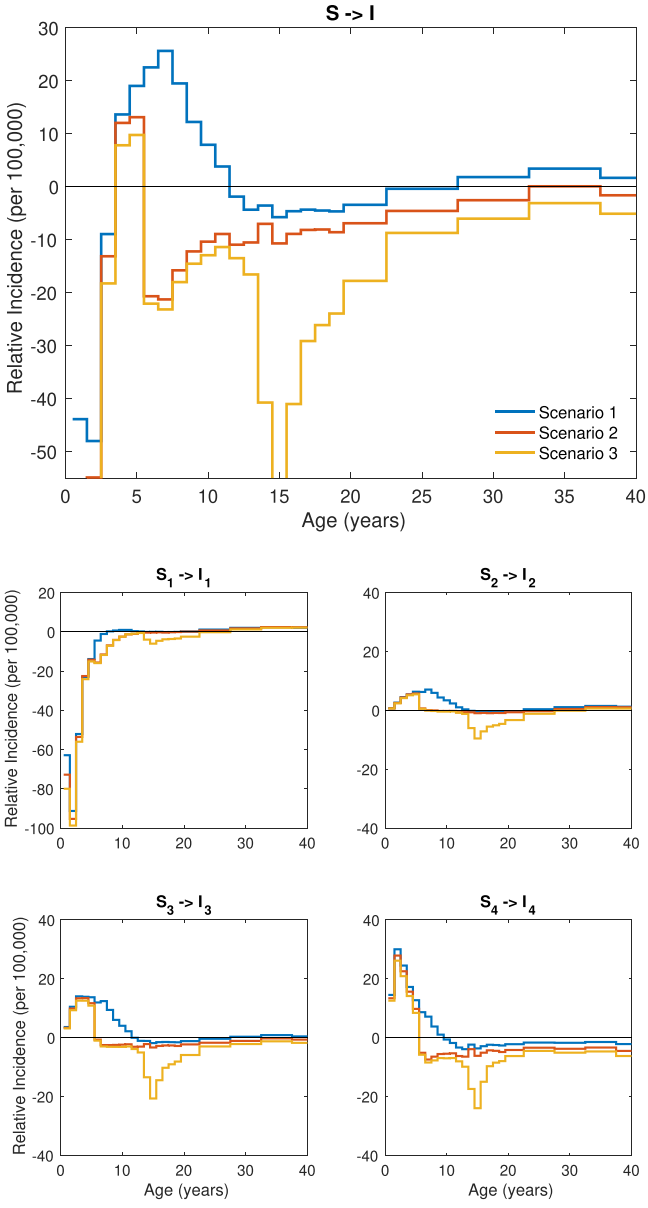

Fig. D.4. Relative change in incidence by age. Comparisons of the incidence of infection by age group under different vaccination strategies: Scenario 1 - primary relative to no vaccination (blue); Scenario 2 - primary vaccination with a single booster dose relative to no vaccination (red); and Scenario 3 - primary vaccination with both booster doses relative to no vaccination (orange). The large panel is a composite of the smaller ones, which are for individual S classes. Negative values on the y-axis indicate a reduction in incidence. In contrast to Fig. 3, the baseline of comparison is absence of vaccination. (For interpretation of the references to colour in this figure legend, the reader is referred to the web version of this article.)

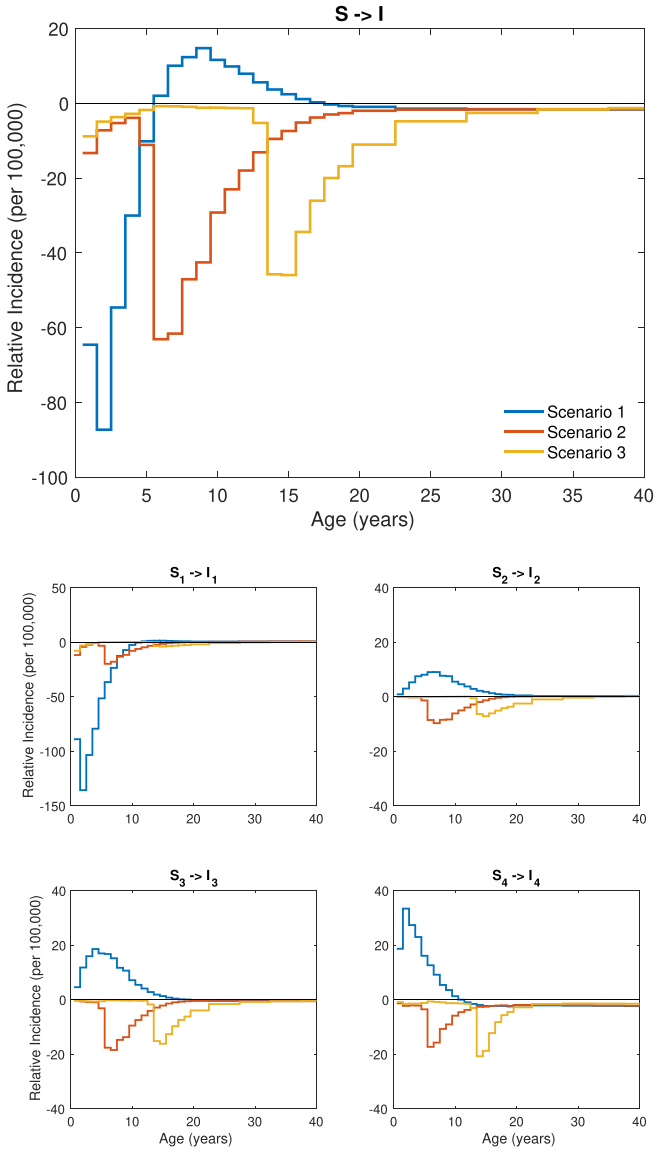

Fig. D.5. Relative change in incidence by age. Comparisons of the incidence of infection by age group under different vaccination strategies: Scenario 1 - primary relative to no vaccination (blue); Scenario 2 - primary vaccination with a single booster dose relative to no vaccination (red); and Scenario 3 - primary vaccination with both booster doses relative to no vaccination (orange). The large panel is a composite of the smaller ones, which are for individual S classes. Negative values on the y-axis indicate a reduction in incidence. In contrast to Fig. 3, proportionate mixing is assumed. (For interpretation of the references to colour in this figure legend, the reader is referred to the web version of this article.)

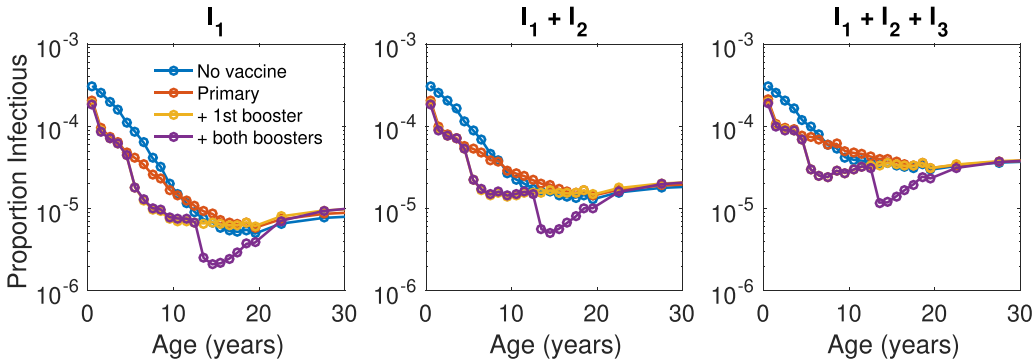

Fig. D.6. Infectious population by symptomatic class under the assumption of proportionate mixing. The proportion of infectious individuals with severe symptoms (A), severe and moderate symptoms (B) or any symptoms (C) under no vaccination (blue), primary vaccination alone (red), primary vaccination with the first booster dose (yellow) and primary vaccination with both booster doses (purple). Note the y-axis log scale. In contrast to Fig. 5, proportionate mixing is assumed rather than the observed mixing matrix. (For interpretation of the references to colour in this figure legend, the reader is referred to the web version of this article.)

Supplementary material

Supplementary material associated with this article can be found, in the online version, at 10.1016/j.jtbi.2020.110265

References

Anderson, R.M., May, R., 1985. Vaccination and herd immunity to infectious diseases. Nature 318, 323.

Águas, R., Gonçalves, G., Gomes, M.G.M., 2006. Pertussis: increasing disease as a consequence of reducing transmission. The Lancet Infectious Diseases 6, 112–117.

Anderson, R.M., May, R.M., 1982. Directly transmitted infections diseases: control by vaccination. Science 215, 1053–1060.

Barbarossa, M.V., Polner, M., Rost, G., 2017. Stability switches induced by immune system boosting in an SIRS model with discrete and distributed delays. SIAM J. Appl. Math. 77, 905–923.

Barbarossa, M.V., Polner, M., Rost, G., 2018. Temporal evolution of immunity distributions in a population with waning and boosting. Complexity 9264743.

Barbarossa, M.V., Röst, G., 2015. Immuno-epidemiology of a population structured by immune status: a mathematical study of waning immunity and immune system boosting. J Math Biol 71, 1737–1770.

van den Driessche, P., Watmough, J., 2002. Reproduction numbers and sub-threshold endemic equilibria for compartmental models of disease transmission. Math. Biosci. 180, 29–48.

Brewer, C. A., 2013. Brewer colormap. http://www.ColorBrewer.org. [Online; accessed 18-March-2018].

Campbell, P.T., McCaw, J.M., McIntyre, P., McVernon, J., 2015. Defining long-term drivers of pertussis resurgence, and optimal vaccine control strategies. Vaccine 33, 5794–5800.

Dafilis, M.P., Frascoli, F., Wood, J.G., McCaw, J.M., 2012. The influence of increasing life expectancy on the dynamics of SIRS systems with immune boosting. The ANZIAM Journal 54, 50–63.

Diekmann, O., de Graaf, W., Kretzschmar, M., Teunis, P., 2018. Waning and boosting: on the dynamics of immune status. J Math Biol 77, 2023–2048.

Feng, Z., Glasser, J.W., 2019. Mixing in meta-population models. The Dynamics of Biological Systems. Springer, Cham., pp. 99–126.

Feng, Z., Glasser, J.W., Hill, A.N., Franko, M.A., Carlsson, R.M., Hallander, H., Tüll, P., Olin, P., 2014. Modeling rates of infection with transient maternal antibodies and waning active immunity: application to bordetella pertussis in Sweden. J. Theor. Biol. 356, 123–132.

Feng, Z., Hill, A.N., Smith, P.J., Glasser, J.W., 2015. An elaboration of theory about preventing outbreaks in homogeneous populations to include heterogeneity or preferential mixing. J. Theor. Biol. 386, 177–187.

Gambhir, M., Clark, T.A., Cauchemez, S., Tartof, S.Y., Swerdlow, D.L., Ferguson, N.M., 2015. A change in vaccine efficacy and duration of protection explains recent rises in pertussis incidence in the United States. PLoS Comput. Biol. 11, e1004138.

Glass, K., Grenfell, B., 2003. Antibody dynamics in childhood diseases: waning and boosting of immunity and the impact of vaccination. J. Theor. Biol. 221, 121–131.

Glasser, J. W., Feng, Z., Moylan, A., Del Valle, S., Castillo-Chavez, C., 2012. Mixing in cross-classified population models of infections diseases. Math Biosci 235, 1–7.

Gustafsson, L., Hallander, H.O., Olin, P., Reizenstein, E., Storsaeter, J., 1996. A controlled trial of a two-component acellular, a five-component acellular, and a whole-cell pertussis vaccine. N top N. Engl. J. Med. 334, 349–356.

Gustafsson, L., Hessel, L., Storsaeter, J., Olin, P., 2006. Long-term follow-up of swedish children vaccinated with acellular pertussis vaccines at 3, 5, and 12 months of age indicates the need for a booster dose at 5 to 7 years of age. Pediatrics 118, 978–984.

Heffernan, J., Keeling, M. J., 2009. Implications of vaccination and waning immunity. Proceedings of the Royal Society of London B: Biological Sciences 1664, 2071–2080.

Hethcote, H., 1997. An age-structured model for pertussis transmission. Math Biosci 145, 89–136.

Hethcote, H., 1999. Simulations of pertussis epidemiology in the united states: effects of adult booster vaccinations. Math Biosci 158, 47–73.

Hethcote, H.W., 2000. The mathematics of infectious diseases. SIAM Rev. 42, 599–653.

Lavine, J.S., King, A.A., Bjørnstad, O.N., 2011. Natural immune boosting in pertussis dynamics and the potential for long-term vaccine failure. Proceedings of the National Academy of Sciences 108, 7259–7264.

Leung, T., Campbell, P.T., Hughes, B.D., Frascoli, F., McCaw, J., 2018. Infection-acquired versus vaccine-acquired immunity in an SIRWS model. Infectious Disease Modelling.

Mims, C.A., Nash, A.A., Stephen, J., 2001. Mims' Pathogenesis of infectious disease. Gulf Professional Publishing.

Mossong, J., Hens, N., Jit, M., Beutels, P., Auranen, K., Mikolajczyk, R., Massari, M., Salmaso, S., Tomba, G.S., Wallinga, J., 2008. Social contacts and mixing patterns relevant to the spread of infectious diseases. PLoS Med. 5, e74.

Mossong, J., Nokes, D.J., Edmunds, W.J., Cox, M.J., Ratnam, S., Muller, C.P., 1999. Modeling the impact of subclinical measles transmission in vaccinated populations with waning immunity. Am. J. Epidemiol. 150, 1238–1249.

Nations, U., 2015. (Accessed june 1, 2018). Demographic Yearbook.

Olin, P., Gustafsson, L., Barreto, L., Hessel, L., Mast, T., Van Rie, A., Bogaerts, H., Storsaeter, J., 2003. Declining pertussis incidence in sweden following the introduction of acellular pertussis vaccine. Vaccine 21, 2015–2021.

Olin, P., Rasmussen, F., Gustafsson, L., Hallander, H.O., Heijbel, H., 1997. Randomised controlled trial of two-component, three-component, and five-component acellular pertussis vaccines compared with whole-cell pertussis vaccine. The Lancet 350, 1569–1577.

Rohani, P., Zhong, X., King, A.A., 2010. Contact network structure explains the changing epidemiology of pertussis. Science 330, 982–985.

Romanus, V., Jonsell, R., Bergquist, S., 1987. Pertussis in Sweden after the cessation of general immunization in 1979. Pediatr. Infect. Dis. J. 6, 364–371.

Storsaeter, J., Hallander, H., Farrington, C.P., Olin, P., Möllby, R., Miller, E., 1990. Secondary analyses of the efficacy of two acellular pertussis vaccines evaluated in a Swedish phase III trial. Vaccine 8, 457–461.

Teunis, P.F.M., Van Der Heijden, O.G., De Melker, H.E., Schellekens, J.F.P., Versteegh, F.G.A., Kretzschmar, M., 2002. Kinetics of the IgG antibody response to pertussis toxin after infection with B. pertussis. Epidemiology of Infection 129, 479–489.

Teunis, P.F.M., van Eijkeren, J.C.H., de Graaf, W.F., Banocic Marinovic, A., Kretzschmar, M.E.E., 2016. Linking the seroresponse to infection to within-host heterogeneity in antibody production. Epidemics 16, 33–39.

Trollfors, B., Taranger, J., Lagergaard, T., Lind, L., Sundh, V., Zackrisson, G., Lowe, C.U., Blackwelder, W., Robbins, J.B., 1995. A placebo-controlled trial of a pertussis–toxoid vaccine. N top N. Engl. J. Med. 333, 1045–1050.